5-2016

Endothelialization and In Vitro Characterization of a Small Diameter Tissue Engineered Vascular Graft for Patients with Diabetes

Eric Brandon Wright
Clemson University, ebwrigh@g.clemson.edu

ENDOTHELIALIZATION AND IN VITRO CHARACTERIZATION OF A SMALL-DIAMETER TISSUE ENGINEERED VASCULAR GRAFT FOR PATIENTS WITH DIABETES

A Thesis
Presented to
the Graduate School of
Clemson University

In Partial Fulfillment
of the Requirements for the Degree
Master of Science
Bioengineering

---

by
Eric Brandon Wright
May 2016

Accepted by:
Dr. Agneta Simionescu, Committee Chair
Dr. Dan Simionescu
Dr. Naren Vyavahare

ABSTRACT

Prosthetic vascular grafting is largely successful in patients undergoing surgical intervention for vascular diseases in medium and large caliber arteries (inner diameter >6 mm). In small diameter arteries, however, prosthetic grafts are insufficiently non-thrombogenic, and autologous vein grafting and endovascular stenting are considered to be standard treatments. However, up to one third of patients lack proper donor vessels due to donor site morbidities or severe vascular disease, and stenting fails to provide long-term patency. Further, patients with diabetes have not only increased risk for the development of cardiovascular diseases, but also have poorer outcomes following intervention. To meet this need, a small diameter tissue engineered vascular graft was developed to meet the needs of diabetic patients with vascular diseases.

First, a biocompatible scaffold was created by decellularization of porcine renal arteries, then stabilizing the scaffolds using pentagalloyl glucose (PGG). PGG is a matrix-binding polyphenol previously shown to improve mechanical strength of decellularized tissues and to resist calcification and the accumulation of advanced glycation endproducts in STZ-induced type I diabetic rats. Decellularization was assessed by histological analysis and isolation and quantification of DNA.

Next, human adipose derived stem cells (hADSC) were differentiated in vitro to endothelial cells in media supplemented with vascular endothelial growth factor (VEGF) and insulin-like growth factor (IGF-1). ADSC-derived endothelial cells and human aortic endothelial

cells (hAEC) were cultured in normal or high glucose for one week. Cells were assessed by immunofluorescence to confirm differentiation toward endothelial cells. Protein and RNA isolates were assessed for the expression of metabolic and inflammatory markers for diabetes to measure the resistance of differentiated hADSCs to a high glucose environment compared to hAEC.

Finally, hAEC and human aortic adventitial fibroblasts (hAAFb) were drop-seeded onto the prepared scaffolds and conditioned in a custom-designed vascular bioreactor in normal or high glucose media for 4 weeks. Constructs explanted from the bioreactors were assessed for cell retention by Live/Dead Assay, scanning electron microscopy, and histology. Protein and RNA isolates were assessed for the same metabolic and inflammatory markers for diabetes.

Histological analysis and DNA concentration showed complete decellularization of porcine renal arteries. A pilot study to assess the *in vitro* response of endothelial-differentiated hADSCs to diabetic conditions was similar to that of hAEC. Decellularized arterial scaffolds seeded with fibroblasts and endothelial cells conditioned in a bioreactor retained some endothelial cells, but lacked fibroblasts after conditioning.

DEDICATION

To my family, who have taught me that education and mindfulness are the keys to happiness and a good life, and to my friends, who remind me every day why life is so great.

ACKNOWLEDGMENTS

I have had an incredible amount of support on this project. Above all, Dr. Agneta Simionescu has provided all that I need to be successful.

I would like to thank my lab mates, the members of the Cardiovascular Tissue Engineering and Regenerative Medicine Lab (CTERM) and the Biocompatibility and Tissue Regeneration Lab (BTRL), for their mentorship and friendship. Particularly, Jhilmil Dhulekar, Dr. Jason Schulte, Dr. Leslie Sierad, Laura McCallum, Christopher DeBorde, Dr. Mike Jaeggli, and Elizabeth Fontaine have given me more help than I can return the favor for.

I would like to thank the Clemson University Department of Bioengineering. For the past 6 years, this department has cultivated me and given me a powerful foundation upon which I can build my career as a bioengineer. Thank you to all of my professors. Even more, departmental staff are knowledgeable and wonderful. Thanks to Cassie Gregory, Maria Torres, Chad McMahan, Linda Jenkins, Leigh Humphries, and Michelle Kirby.

Finally, I would like to thank the National Institutes of Health and SCBIOCRAFT for funding via the 5P20GM103444-07 5535 grant.

TABLE OF CONTENTS

Page

Table of Contents (cont.) Page

Table of Contents (cont.) Page

LIST OF TABLES

LIST OF FIGURES

List of Figures (Cont.)

Page

CHAPTER ONE: BACKGROUND AND REVIEW OF LITERATURE

1.1 Cardiovascular Anatomy and Physiology

1.1.1 Overview of the Cardiovascular System

At its core, the cardiovascular system exists to conduct blood in a closed loop throughout the body. The center of this system is the heart, a four-chambered organ organized to create continuous, unidirectional flow of blood. In the pulmonary circuit, blood is pumped from the right ventricle through the pulmonary arteries to the lungs, wherein oxygen and carbon dioxide are exchanged with atmospheric gas, then the re-oxygenated blood returns through the left atrium. Once full, the atrium contracts to send blood into the left ventricle, which then pumps blood to the aorta, which has a series of branches coming off it to allow blood to travel throughout the body. At the periphery, nutrients, waste, gases, and hormones are exchanged in thin-walled capillaries. Blood then returns to through the venous system to the right atrium, and the cycle thus continues.

1.1.2 The Vasculature

Blood vessels are the conduits by which blood is conducted throughout the body. It is divided into three subtypes: arteries, veins, and capillaries. Additionally, smaller vessels called arterioles and venules to act as intermediate-sized vessels to connect capillaries to arteries and veins, respectively. The vessels are generally composed of endothelial and smooth muscle cells and extracellular matrix, primarily collagens, elastin, and glycosaminoglycans. Arteries and veins are multi-layered organs: the innermost, blood-contacting layer is the tunica intima, also referred to as the endothelium, consists of a

monolayer of endothelial cells, a specialized type of epithelial cell, on top of a basement membrane. The tunica media is separated from the endothelium by an internal elastic lamina, forms the middle layer of blood vessels, and is composed of concentric layers of vascular smooth muscle cells (vSMC). The tunica externa is the outmost layer, and is separated from the media by external elastic lamina.[26] It a loose connective tissue containing nerve endings and in larger vessels, a vasa vasorum[26], a network of arterioles and capillaries that nourish the outermost parts of those vessels. Capillaries consist of a monolayer of endothelial cells on a basement membrane.

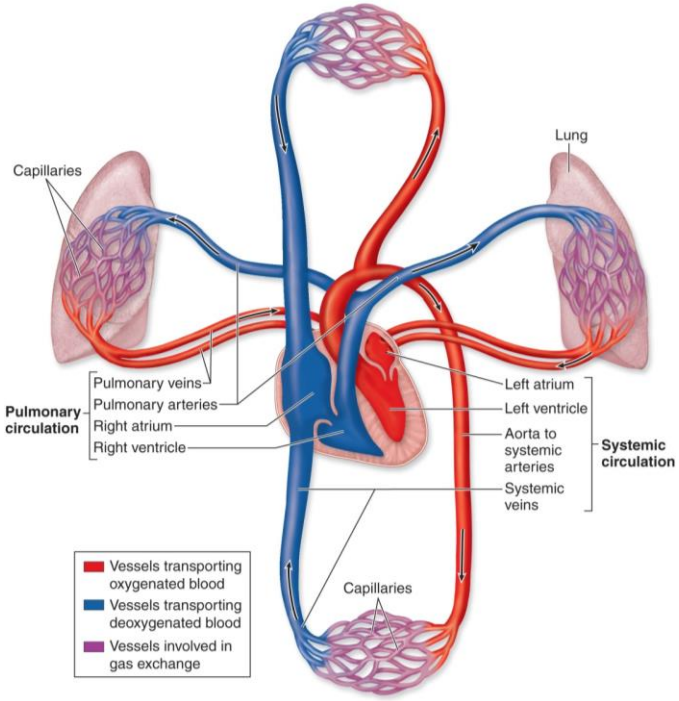

Figure 1.1: The Cardiovascular System. The system is composed of the heart, the pulmonary circuit, which supplies the lungs, re-oxygenates blood, and removes waste carbon dioxide, the system circuit, which supplies blood to all other parts of the body besides the lungs. Oxygenated blood is depicted in red and deoxygenated blood is depicted in blue. [25]

Generally, arteries have thicker vessel walls and narrower lumens to compensate for greater mean pressure and flow rate. The largest arteries are those closest to the heart, and have inner diameters between 1 and 2.5 cm.[25] These arteries have the highest elastin content, which allows for the arterial wall to stretch and recoil following a pulse of blood without permanent deformation while damping the pulsation generated by the cardiac rhythm; thus they are referred to as elastic arteries.[31] Muscular arteries are slightly smaller than elastic arteries, with diameters between 3 mm and 1 cm.[25] As the name suggests, these arteries have a proportionally thicker tunica media, which is stimulated by the endothelium or the nervous system to induce vasoconstriction or vasodilation in order to reduce to increase blood, respectively, to a given organ or tissue. Veins have much wider lumens and thinner walls than their companion arteries. This is because of the lower pressure experienced after flow through capillaries. This low pressure also means that blood flow is able to stop. To prevent blood from pooling in the peripheral veins, particularly in the limbs, veins have valves to prevent backflow, and deep veins lie next to skeletal muscles, which act to pump blood back toward the heart.[25]

1.1.3 The Endothelium

Endothelial cells are a specialized squamous epithelium form a 0.2-0.4 μm -thick monolayer of cells that line the luminal of surface of all vasculature and the heart[10], and are key regulators of vascular wall homeostasis.[38] With the exceptions of fenestrated endothelium in the hepatic and splenic vasculature, endothelial cells form a tight, selectively permeable barrier. Endothelial cells are highly dynamic and can change

phenotype based on homeostatic signaling. Under normal homeostatic conditions, endothelial cells form a barrier between the blood compartment and extravascular tissues, resist thrombogenesis, prevent immune cell extravasation, regulate vascular tone, and favor overturn of vascular extracellular matrix.[26]

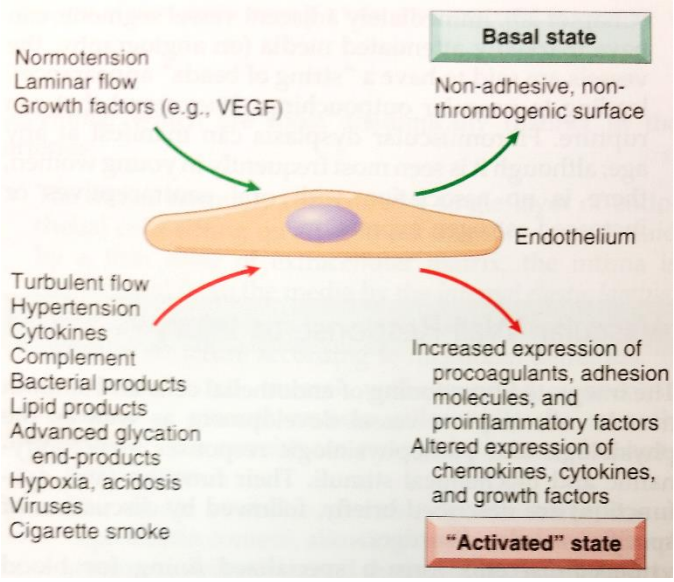

Figure 1.2: Activation of Endothelial Cells [26]

Under various states of stress, including turbulent flow, hypertension, cytokines, complement activation, damage from hyperglycemia, hypoxia, acidosis and alkalosis, endothelial cells become activated.[26] Activated endothelial cells become procoagulant, proinflammatory, and influence the underlying smooth muscle cells to contract and proliferate. These functions allow for hemostasis, inflammatory cell recruitment to combat infection, and intimal thickening to allow for vessel healing.[26] This activated state is contrasted with endothelial dysfunction, a proinflammatory and procoagulant phenotype that forms the basis of various vascular disorders, including thrombosis, atherosclerosis,

and vascular lesions caused by hypertension and other disorder.[24] Generally, endothelial dysfunction is a phenotypical alteration that leads to loss of homeostatic control and contributes to the pathogenesis of vascular diseases, including thrombosis, atherosclerosis, and vascular lesions seen in hypertensive patients.[10,26,33]

1.1.3.1 Endothelial Regulation of Hemostasis

Under normal conditions, endothelial cells express anti-platelet, anti-coagulation, and fibrinolytic factors that contribute to the total non-thrombogenicity of the tunica intima.[38] Endothelial cells constitutively express prostaglandin 2 (PGI_2) and endothelial nitric oxide synthase (eNOS) to prevent adhesion of platelets to the vascular wall.[10] PGI_2 exerts a paracrine effect on platelets and nearby endothelial cells. In platelets, PGI_2 inhibits thromboxane A2 (TXA2) synthesis, which is necessary for platelet activation and aggregation.[10] eNOS catalyzes the reaction that produces nitric oxide (NO). NO inhibits P-selectin expression and integrin glycoprotein IIb-IIIa activation in platelets, which are necessary for platelet aggregation and fibrinogen binding, respectively.[10] Endothelial cells inhibit coagulation by releasing a variety of factors that inhibit the various parts of the coagulation cascade and fibrin clot formation. Finally, endothelial cells express tissue plasminogen factor (tPA), a fibrinolytic enzyme involved in clot dissolution.[33] Upon activation, endothelial cells suppress their anti-thrombogenic phenotype and release tissue factor, an enzyme that catalyzes cleavage of Factors IX and X to aid in coagulation cascade progress.[33]

1.1.3.2 Endothelial Regulation of Immune Response

In addition to inhibiting platelet adhesion, endothelial cells ensure that immune cells, especially leukocytes and monocytes, cannot bind to the vascular wall and enter the extravascular tissue. The endothelium does this by passively failing to produce the requisite chemoattractant and adhesive molecules necessary to mediate leukocyte recruitment.[33] Upon activation, endothelial cells produce cytokines that activate leukocytes, chemokines that recruit monocytes to the area of injury, and express surface adhesive molecules that allow immune cells to bind to the vascular wall. Early adhesion to the vascular wall is mediated by E-selectin, giving leukocytes low-affinity binding.[6] Immune cells will then transiently "roll" along the vascular wall. Immune cells express integrins that bind to intracellular adhesion molecules (ICAMs) and vascular CAMs (VCAMs) expressed on the luminal surface of activated endothelial cells.[6] Integrin-mediated binding allows for firm attachment to the vascular wall, and induces rapid cytoskeletal remodeling within the immune cells, which allows them to extravasate to the tissue bed by "squeezing" themselves through gaps between the endothelial cells in a process called diapedesis or transendothelial migration.[6]

1.1.3.3 Endothelial Regulation of Vascular Tone

Blood pressure is regulated by two key functions: cardiac output and peripheral resistance.[26] Cardiac output is affected by stroke volume and heart rate. Peripheral resistance is primarily regulated by vascular tone at the arteriole level, and is balanced by levels of vasoconstrictors and vasodilators, many of which are produced by endothelial

cells.[26] In addition to their roles as a platelet activation inhibitors, NO and PGI_2 are potent vasodilators. Endothelial cells constitutively express eNOS, which continuously produced NO. Additional large levels of NO can be produced by and inducible nitric oxide synthase (iNOS), which is activated in macrophages, SMCs, and endothelial cells in response to cytokine signaling.[33] PGI_2 and TXA2 are vascular tone antagonists, inducing vasodilation and vasoconstriction, respectively.[33]

During injury, the endothelium contributes to vasoconstriction to aid in prevention of blood loss. Endothelial cells are responsible for the production of endothelin-1 and angiotensin II by the actions of endothelin converting enzyme and angiotensin converting enzyme (ACE) on the cell membrane.[33] Endothelin-1 is released abluminally to stimulate SMC contraction.[10] Angiotensin II is the end product of the renin-angiotensin system that controls blood pressure by inducing vSMC contraction, stimulating aldosterone secretion by the adrenal glands to resorb filtered sodium, stimulating vasopressin secretion by the posterior pituitary gland to increase fluid retention in the kidneys, and inhibiting bradykinin, a vasodilator that induces NO and PGI_2 release from endothelial cells.[10,26,33]

1.2 Cardiovascular Disease and Current Treatments

1.2.1 Incidence of Cardiovascular Disease

Cardiovascular diseases are the leading cause of morbidity and mortality in the world, and in the United States in 2011, accounted for 31.3% of deaths.[27] These diseases include stroke, congenital heart disease, rhythm disorders, atherosclerosis, heart failure, valvular

disease, coronary artery disease, and peripheral artery disease.[27] The focus of this review will be on macrovascular diseases, especially coronary, carotid, and peripheral artery diseases. Coronary artery disease (CAD) affects 6.2% (15 million) of the U.S. population, and is a significant risk factor in the development of heart failure and myocardial infarction.[27] Peripheral artery disease (PAD) affects 3.5% (8.5 million) of the U.S. population[27], and characterized by claudication, intermittent leg pain during physical activity. Left untreated, PAD can cause critical limb ischemia, which may require lower extremity amputation.

1.2.2 Atherosclerosis

Vascular pathologies are underpinned by two principle mechanisms, stenosis of the vessel that leads to obstruction of the vessel, and weakening of the vessel wall that can lead to dilation and eventual rupture.[26] One of the mechanisms leading to vessel obstruction is arteriosclerosis, i.e. hardening of the arteries, which has three general manifestations: 1) arteriolosclerosis, which primarily affects small arteries and arterioles, 2) Mönckeberg medial sclerosis, dystrophic calcification in the tunica media of muscular arteries, and 3) atherosclerosis, deposition of a fatty plaque in the vessel wall.[26] Atherosclerosis is the leading cause of morbidity and mortality in Western countries, and will be the focus of this review.

The most common model for describing atherogenesis, the pathogenesis of atherosclerosis, is the response-to-injury hypothesis[34], which "views atherosclerosis as a chronic

inflammatory and healing response of the arterial wall to endothelial injury."[26] First, endothelial cells experience chronic injury, particularly from hyperlipidemia and disturbed mechanical forces, leading to endothelial dysfunction that manifests in increased vascular permeability, leukocyte adhesion and extravasation, and thrombosis.[34] Next, low density lipoprotein (LDL) and oxidized LDL begin to accumulate in the vascular wall. Monocytes then adhere, migrate into the vessel wall, and transform into macrophages. Smooth muscle cells also migrate into the intima in response to the vessel injury. Macrophages and SMCs begin accumulating deposited lipids, and macrophages transform into foam cells due to modified LDL ingested via scavenger receptors; this stage is referred to as a fatty streak.[26,41] Macrophages are activated by uptaken cholesterol and free fatty acids (FFA) that interact with components of the inflammasome[20] that enhances immune cell recruitment via cytokine release, increased lipid oxidation and oxidative stress via release of radical oxygen species (ROS), and SMC proliferation via growth factor release.[26] Activated T lymphocytes release interferon-γ (IFNγ), which activates macrophages, SMCs, and endothelial cells.[20] Activated and proliferative intimal SMCs have a unique synthetic phenotype, in which they deposit ECM components, particularly collagen, which completes transformation of the fatty streak into a fibrofatty atheroma.[26] This fibrofatty atheroma is commonly referred to as an atherosclerotic plaque. Cell necrosis within the plaque contributes to degeneration of the underlying intima, resulting in a vulnerable plaque that can lead to clinically relevant consequences.[26]

At the clinical stage, there are several important pathologic consequences. Acute changes in the surface of the plaque can lead to rupture, ulcerate, or erode, exposing the highly thrombotic interior of the plaque to the bloodstream and thus resulting in acute vessel occlusion.[26,42] The plaque can weaken the surrounding vessel wall due to intimal ischemia and ECM degradation, which can induce aneurysm formation that may rupture. In small arteries, plaques can become large enough to occlude the vessel, resulting in downstream ischemia.[4] At the clinical stage, there are several interventions, including pharmacotherapy, balloon angioplasty, stenting, and bypass graft surgery.[7,36]

Type of lesion	Subtype of lesion	Morphological description
Nonatherosclerotic intimal lesions	Intimal thickening	Natural accumulation of smooth muscle cells in the absence of lipid, macrophage foam cells, and thrombosis.
	Intimal xanthoma	Superficial accumulation of foam cells without a necrotic core, fibrous cap, or thrombosis.
Progressive atherosclerotic lesions	Pathological intimal thickening	Plaque rich in smooth muscle cells, with hyaluronan and proteoglycan matrix and focal accumulation of extracellular lipid. Absence of thrombosis.
	Fibroatheroma	During early necrosis: focal macrophage infiltration into areas of lipid pools with an overlying fibrous cap. During late necrosis: loss of matrix and extensive cellular debris with an overlying fibrous cap. With or without calcification. Absence of thrombosis.
	Intraplaque haemorrhage or plaque fissure	Large necrotic core (size >10% of plaque area) with haemorrhage, and plaque area shows presence of angiogenesis. Necrotic core communicates with the lumen through a fissure. Minimal tear without obvious thrombus.
	Thin-cap fibroatheroma	A thin, fibrous cap (<65 μm) infiltrated by macrophages and lymphocytes, with rare or no smooth muscle cells and relatively large underlying necrotic core (>10% of plaque area). Intraplaque haemorrhage and/or fibrin might be present. Absence of thrombosis.
Lesions with acute thrombi	Plaque rupture	Thin-cap fibroatheroma with cap disruption. Thrombosis is present and might or might not be occlusive. The luminal thrombus communicates with the underlying necrotic core.
	Plaque erosion	Can occur on pathological intimal thickening or on a fibroatheroma. Thrombosis is present and might or might not be occlusive. No communication of the thrombus with the necrotic core.
	Calcified nodule	Eruptive (shedding) of calcified nodule with an underlying fibrocalcific plaque with minimal or no necrosis. Thrombosis is usually not occlusive.
Healed lesions	Healed plaque rupture, erosion, or calcified nodule	Healed lesion composed of smooth muscle cells, proteoglycans, and collagen type III with or without underlying disrupted fibrous cap, necrotic core, or nodular calcification. Lesions can contain large areas of calcification with few inflammatory cells and have a small or no necrotic core. The fibrotic or fibrocalcific collagen-rich plaque is associated with significant luminal stenosis. Absence of thrombosis.

Table 1.1: Classification of atherosclerotic plaques based on morphology [42]

1.2.3 Endovascular Repair

Since the introduction of balloon angioplasty in 1979[19], there have been several generations of technologies to improve the outcomes of percutaneous coronary interventions (PCI), including bare metal stents (BMS) and 1st and 2nd generations of drug-eluting stents (DES). Balloon angioplasty is now the first step in PCI, and involves catheterization in the coronary and expansion of a balloon that compresses the atherosclerotic plaque against the vascular wall. This immediately restores blood flow to the area of ischemia, but restenosis occurs in 50% of patients following balloon angioplasty.[19] Restenosis is clinically defined as >50% vessel occlusion;[19] due to the fourth power relation between tube diameter and conductance, this corresponds to a 94% reduction in flow rate. Endovascular surgeries cause localized trauma at the site of treatment and can lead to vessel wall spasm or thrombosis,[27] and the vessel wall elastically recoils following balloon angioplasty.[36]

To combat elastic recoil, bare metal stents were introduced in the late 1980s[19], and stenting is now practiced in 90% of PCI surgeries.[27] BMS improved restenosis rates to 20-30%[19] at 6-12 months[27], but restenosis occurs due to a different pathology: intimal hyperplasia. Endothelial denudation and exposure of vSMCs due shear stress from blood flow causes SMCs to migrate to the intima, proliferate, and take on a synthetic phenotype similarly seen in atherosclerosis.[19,27,36] Additionally, stenting requires exogenous administration of anti-thrombogenic and anti-platelets pharmaceuticals to address the presence of thrombogenic material exposed to the bloodstream.[13]

As an improvement to bare metal stents, manufacturers began coating stents in anti-proliferative drugs, such as Sirolimus and Paclitaxel, to combat in-stent restenosis.[13,19] These stents improved restenosis rates to 5-15%[19], but anti-proliferative therapies also slow healing of the endothelium, which is necessary to permanently halt SMC proliferation, and after the drug is fully released, DES resemble BMS and a "late catch-up phenomenon"[19] is observed more than a year after initial revascularization.

1.2.4 Vascular Replacement

Synthetic grafts composed of hydrophobic polymers, such as poly (ethylene-terephthalate) (PET) and expanded polytetrafluoroethylene (ePTFE), affixed with metallic struts to resist kinking have largely been successful in large-diameter (>8 mm inner diameter) vascular grafting.[8] Although these materials are not entirely non-thrombogenic, the shear forces in large-diameter arteries, such as the ascending and abdominal aorta, iliac, and femoral arteries, are great enough to inhibit thromboembolism formation; these grafts boast 90% patency rates 5 years after surgery.[8] However, patency rates are as low as 39% at 5 years for the same materials in small-diameter vessels (<6 mm inner diameter), such as the coronary artery and arteries below the knee, compared to 74% in autografts.[8] In addition to insufficient blood flow to overcome graft thrombogenicity, compliance mismatch between the graft and the native artery and flow disturbances contribute to intimal hyperplasia at the distal end of the graft.[36] 5-year patency rates are similar between synthetic and autologous grafts for medium-caliber arteries (6-8 mm inner diameter).[8]

The first successful attempt at vascular intervention was the use of an autologous saphenous vein graft for a femoropopliteal bypass in 1948.[36] Autologous vessel grafting is now considered the gold standard in vascular intervention.[8,36] The saphenous vein is the most commonly used autograft due to length and ease of access[36], and the internal mammary and radial arteries are also commonly used.[8] The saphenous vein, however, is considered an inferior choice, and has a 10-year patency rate of 50% due to the mechanical mismatch of a new high-flow environment that leads to aneurysm, intimal hyperplasia, and atherosclerosis in the graft.[36] Internal mammary arteries, on the other hand, have 10-year patency rates greater than 90%. Unfortunately, one-third of patients lack sufficient donor grafts due donor site morbidity, prior vessel harvesting, or anatomical suitability.[8]

1.2.5 The Need for a Tissue Engineered Vascular Graft

Due to high rates of revision surgeries, insufficient long term patency, inadequate performance of synthetic grafts, and insufficient access to donor grafts, there is a need for an alternative solution for revascularization surgeries. With advances in material science and cell biology, tissue engineering has shown great promise to meet this need. The goal of developing a tissue engineered vascular graft is to mimic the properties and geometry of the native vessel being replaced. Ideally, such a graft would match mechanical strength and compliance, be non-toxic and non-immunogenic, be non-thrombogenic, be easy to handle and suture, have reasonable costs and batch consistency in manufacturing, and totally integrate with the host tissue, including the ability to grow when implanted in pediatric patients.[8,27,36]

1.3 Impact of Diabetes Mellitus in Cardiovascular Disease

1.3.1 Characterization of Diabetes Mellitus

Diabetes mellitus (DM) is a chronic metabolic disease characterized by dysregulation of blood glucose levels.[29] DM generally falls into three categories. In type I diabetes, previously known as juvenile-onset diabetes because peak diagnosis age occurs in the mid-teens, is the result of autoimmune attack on the β cells of the pancreatic islets, which are responsible for insulin secretion. This leads to the inability to mediate hyperglycemia, and thus patient survival requires regimented exogenous administration of insulin. Type I DM is the most severe form of diabetes and accounts for about 5% of diagnosed cases of diabetes.[28] Type II DM, formerly known as adult-onset diabetes due to the later onset than type I DM, is typically brought on by progressive insulin resistance, insufficient production of insulin by the pancreatic islets, or both and represents 90 to 95% of diabetes cases.[28] Gestational diabetes is a form of glucose intolerance reported in 5 to 10% of pregnant women often diagnosed in the second or third trimester. Gestational diabetes has similar risk factors to those of type II DM, and can itself be a risk factor for gestational diabetes in future pregnancies or the development of type II diabetes.[28]

Diagnosis of diabetes is based on four criteria: 1) fasting plasma glucose ≥126 mg/dL, 2) random plasma glucose ≥200 mg/dL in patients experiencing classic hyperglycemic signs, 3) plasma glucose ≥200 mg/dL following an oral dose of 75 g glucose (oral glucose tolerance test, OGTT), and 4) glycated hemoglobin (Hb_{A1C}) ≥6.5%.[23] The first, third, and

fourth tests are repeated to confirm diagnosis. Patients who do not exhibit outright diabetes can be identified as prediabetic, or having impaired glucose tolerance. The criteria for prediabetes are 1) fasting glucose between 100 and 125 mg/dL, 2) plasma glucose between 140 and 199 mg/mL 2 hours after an OGTT, and 3) Hb_{A1C} between 5.7% and 6.4%.[23]

1.3.2 Incidence and Impact of Diabetes Mellitus

In 2014, 29.1 million people of all ages in the United States had diabetes, accounting for 9.3% of the population.[28] This includes 8.1 million people with undiagnosed diabetes. A further 86 million Americans aged 20 years or older may have prediabetes.[28] There are 387 million people ages 20 to 79 worldwide are estimated to have diabetes in 2014, at 8.3% of the world population.[17] This epidemic is expected to grow to 582 million (10% of the world population) by 2030.[17] Diabetes caused 245 billion USD in direct and indirect costs in the United States in 2012[28], and 612 billion USD worldwide in 2014.[17]

DM is one of the major risk factors for the development of cardiovascular diseases (CVD) and stroke. Patients with diabetes are at a 2- to 4- fold greater risk for developing coronary artery disease (CAD)[27] and a 100-fold greater risk for developing peripheral atherosclerosis-induced gangrene, which requires amputation.[23] While 8.5% of adults in the U.S. in 2012 had diagnosed DM,[2] DM patients represented 27 and 30% of patients undergoing surgical repair for CAD and peripheral vascular disease (PVD), respectively.[27] Cardiovascular diseases include microangiopathies, particularly nephropathy, retinopathy, neuropathy, and impaired wound healing, and macroangiopathies, such as coronary artery

disease, cerebrovascular disease, and peripheral vascular disease.[30] The pathogenesis of CVD in diabetic patients is complex and not yet fully understood, but four distinct mechanisms or pathways have been implicated: advanced glycation endproduct formation, oxidative stress and alteration of the polyol pathway, activation of protein kinase C, and increased hexosamine pathway activity.[18,23,29]

1.3.3 Biochemical Mechanisms of Hyperglycemic Damage

1.3.3.1 Advanced Glycation Endproduct Formation

Advanced glycation endproducts (AGEs) are a heterogeneous group of molecules formed by non-enzymatic reaction between reducing sugars and amino acids.[29] AGEs accumulate naturally during aging, but this process is accelerated in diabetic patients. Glycation occurs via the Maillard reaction, which begins with the spontaneous formation of a Schiff base between the carbonyl groups of glucose or other reducing sugars and a free amino acid.[39] The Schiff base can rearrange to form an Amadori product or fragment as a result of glycoxidation to form reactive intermediates, such as glyoxal (GO), methylglyoxal (MGO), or 3-deoxyglucosone.[39] These reactive dicarbonyl precursors can also be produced by other glycolytic pathways or during lipid peroxidation. Amadori products finally undergo further structural changes via oxidation and degradation to irreversibly form AGEs[39], and dicarbonyl precursors can form AGEs directly.[23] AGE precursors not only alter intracellular proteins, but easily diffuse across the cell membrane, where they can modify extracellular matrix proteins and circulating blood proteins.[39] The glycation of biological molecules by glucose and other sugars alters their function, leading to a wide array of

consequences.

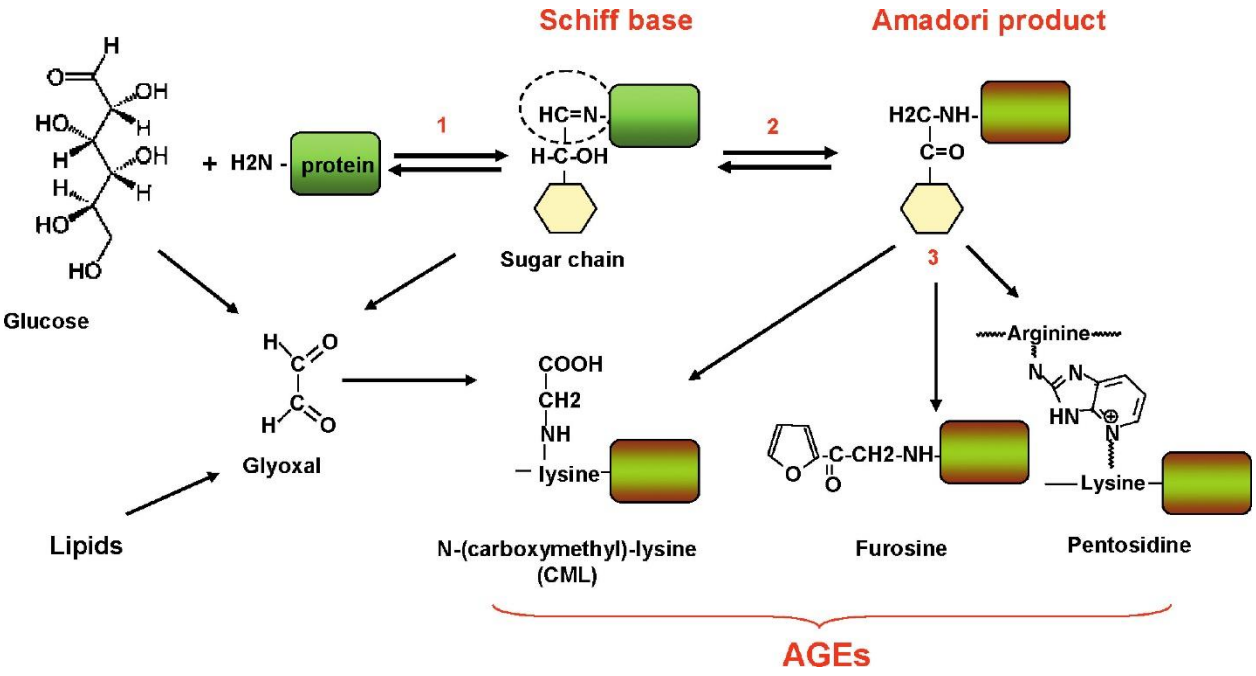

Figure 1.3: The Maillard Reaction leads to the formation of AGE production first by reversible interaction between the carbonyl group of a reducing sugar with amino groups of proteins to form a Schiff base. This is followed by glycoxidation of the sugar side chain to form a dicarbonyl or further rearrangement to form an Amadori product. Amadori products can undergo irreversible oxidation, dehydration, or degradation to form an AGE. Dicarbonyls can form AGEs directly. [30]

First, glycation of intracellular proteins leads to increased proteosomal degradation, altered cell signaling, and altered gene expression, all of which can lead to aberrant cell function or cell death. AGEs can directly cross-link ECM proteins[23], especially collagens.[39] Cross-linking of collagens type I and type IV in the vascular bed causes a decrease in vessel elasticity, thereby increasing wall shear stress, and decreasing endothelial cells adhesion to

the basement membrane, respectively, and thus contributes to endothelial dysfunction.[40] Further, ECM protein cross-linking increases proteolytic degradation and impairs matrix-cell signaling.[23,39] Finally, glycated circulating blood proteins induce pro-inflammatory signaling and oxidative stress via interaction with receptors for AGEs (RAGE) expressed by endothelial cells, vascular smooth muscle cells, and inflammatory cells (macrophages and T lymphocytes).[23,39]

The AGE-RAGE signaling axis results in a variety of effects. Most of these effects are thought to occur via NAPDH oxidase (NOX) -dependent activation of NF-κB, leads to an inflammatory response.[23] Endothelial activation from AGE-RAGE signaling includes increased expression of adhesion molecules (selectins, VCAM-1, ICAM-1), which allows for increased recruitment of leukocytes and monocytes, and increased expression of endothelin-1 and decreased eNOS, causing increased vasoconstriction and impaired vasodilation, respectively, that contributes to hypertension.[4,29] Signaling from glycated LDL and albumin stimulates expression of inflammatory cytokines (TNF-α, IL-1, IL-6) that increase activation of pro-inflammatory cells, MMPS-1, -2, -3, and -13, and chemokines that increase inflammatory cell recruitment.[29] Further, RAGE is upregulated in the cells of DM, thus further accelerating the damaging effects of AGE formation.[21] This milieu of events lead to increased inflammatory cell recruitment, extravasation to the vascular bed, uptake of glycated and glycoxidized LDLs, which have significantly increased levels in diabetic patients, via scavenger receptors, foam cell formation, and growth of fatty streaks.[18,29] These factors contribute to the accelerated atherogenesis seen

in diabetic patients.

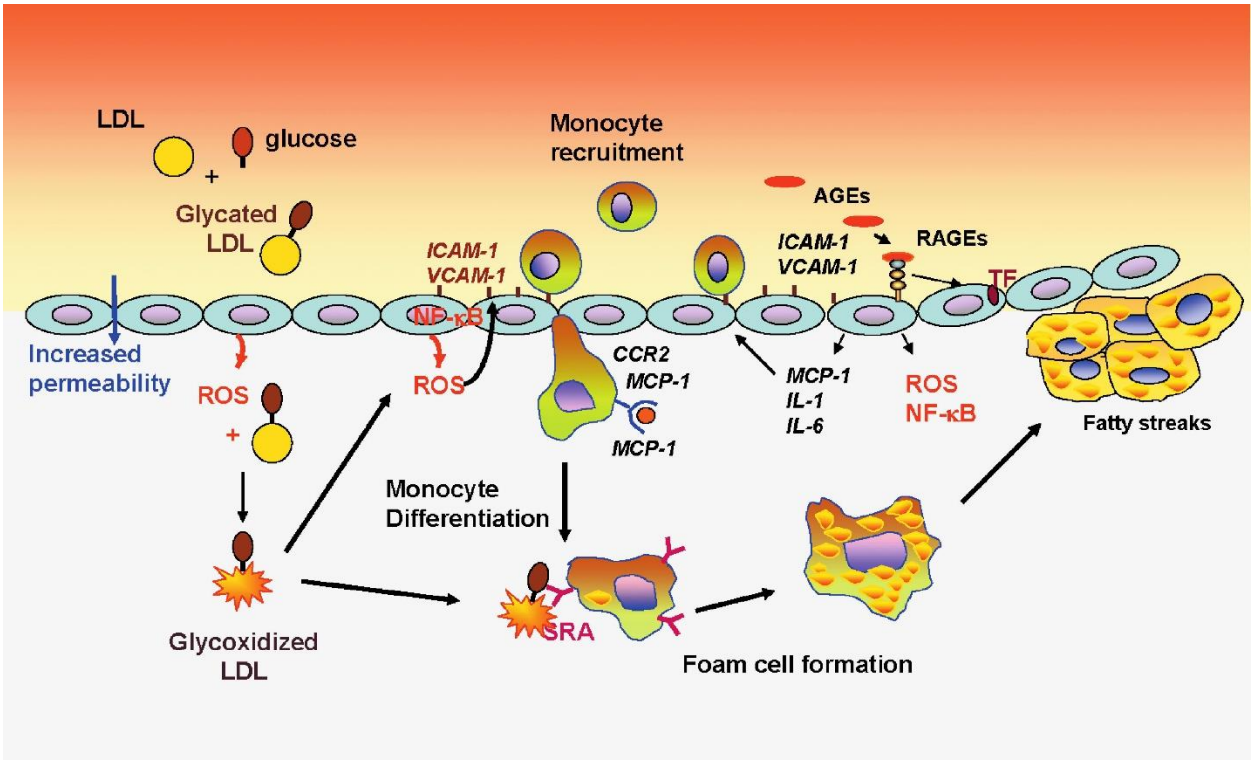

Figure 1.4: The AGE-RAGE signaling axis induces an oxidative stress and pro-inflammatory environment which contributes to accelerated atherogenesis in diabetic patients [30]

1.3.3.2 Oxidative Stress and the Polyol Pathway

Oxidative stress in DM is induced by concomitant increased production of reactive oxygen species (ROS) and decreased activity of molecular antioxidants in concert with increased blood glucose. The most damaging effects of diabetic oxidative stress are seen in cells that are unable to regulate intracellular glucose levels and generate high levels of ROS during hyperglycemia, especially endothelial cells, mesangial cells of the kidney, neurons and neuroglia, and pancreatic β cells.[29] ROS are produced as normal byproducts of cellular

metabolism by the mitochondrial respiratory chain and various oxidative enzymes by cells of the innate immune system as a defense against pathogens. Although the production of ROS is a natural process, their presence can lead to pathologic effects if unchecked. These include lipid peroxidation, leading to membrane degradation, protein modifications that lead to misfolding or impaired function and increased proteosomal breakdown, and single- and double-stranded breaks in DNA, which can result in mutations.[23] These effects are collectively referred to as oxidative stress. To combat these effects, cells have numerous mechanisms to scavenge free radicals. These include antioxidant molecules that block free radical formation or scavenge free radicals, such as retinol, β-carotene, tocopherols, ascorbic acid, and glutathione, and scavenger enzymes, including superoxide dismutase, catalase, and glutathione peroxidase.[23] Should an imbalance between ROS production and scavenging activity arise, oxidative stress ensues.

During DM, excess glucose oxidized in the tricarboxylic acid cycle increases the amount of electron donors pushed through the electron transport chain of the mitochondrial membrane.[4,29] This results in a "back-up" in electron transfer and subsequent donation of electrons to molecular oxygen and the formation of superoxide ($O_2^{\bullet -}$), a potent ROS normally degraded to peroxide by superoxide dismutases (SOD).[23] Further, aldose reductase, an enzyme which has the normal function of reducing aldehydes to less toxic alcohols, metabolizes excess intracellular glucose to sorbitol, a polyol.[23] This process requires consumption of NADPH, which is a critical cofactor for restoring reduced glutathione (GSH), a key intracellular antioxidant.[10] These are keys examples of how DM

induces an imbalance between ROS production and scavenging.

1.3.3.3 PKC Activation

PKC activation due to increased intracellular glucose leads to a variety of altered signaling pathways, resulting in downregulation of endothelial nitric oxide synthase (eNOS), upregulation of endothelin-1, transforming growth factor β (TGF-β), and plasminogen activator inhibitor-1 (PAI-1), and activation of NF-κB and NADPH oxidase (NOX) by vascular endothelial growth factor (VEGF), among others.[29] These lead to decreased vasodilation and hypertension (eNOS and endothelin-1, respectively), proinflammatory signaling (NF-κB), oxidative stress (NOX), increased recruitment of monocytes (VCAMs, ICAMs), and decreased fibrinolysis (PAI-1).[4,29] This signaling cascade, leads to accelerated atherogenesis in diabetic patients, thus contributing to the increased rate of macroangiopathies in those patients.

1.3.3.4 The Hexosamine Pathway

In the first steps of glycolysis, glucose is converted to glucose-6-phosphate, and then into fructose-6-phosphate.[24] From there, the glycolytic pathway can continue, or fructose-6-phosphate can be diverted in the hexosamine signaling pathway, in which some fructose-6-phosphate is enzymatically converted into *N*-acetylglucosamine, which participates in O-linked glycosylation of serine and threonine residues as a part of signal cascade propagation.[4,29,] In DM, excess glucosamine is produced and in particular, overmodification of the transcription factor Sp1 leads to upregulation of TGFβ-1 and PAI-

1 expression.[4,29] These exacerbate fibrosis in the vascular walls of diabetic patients.

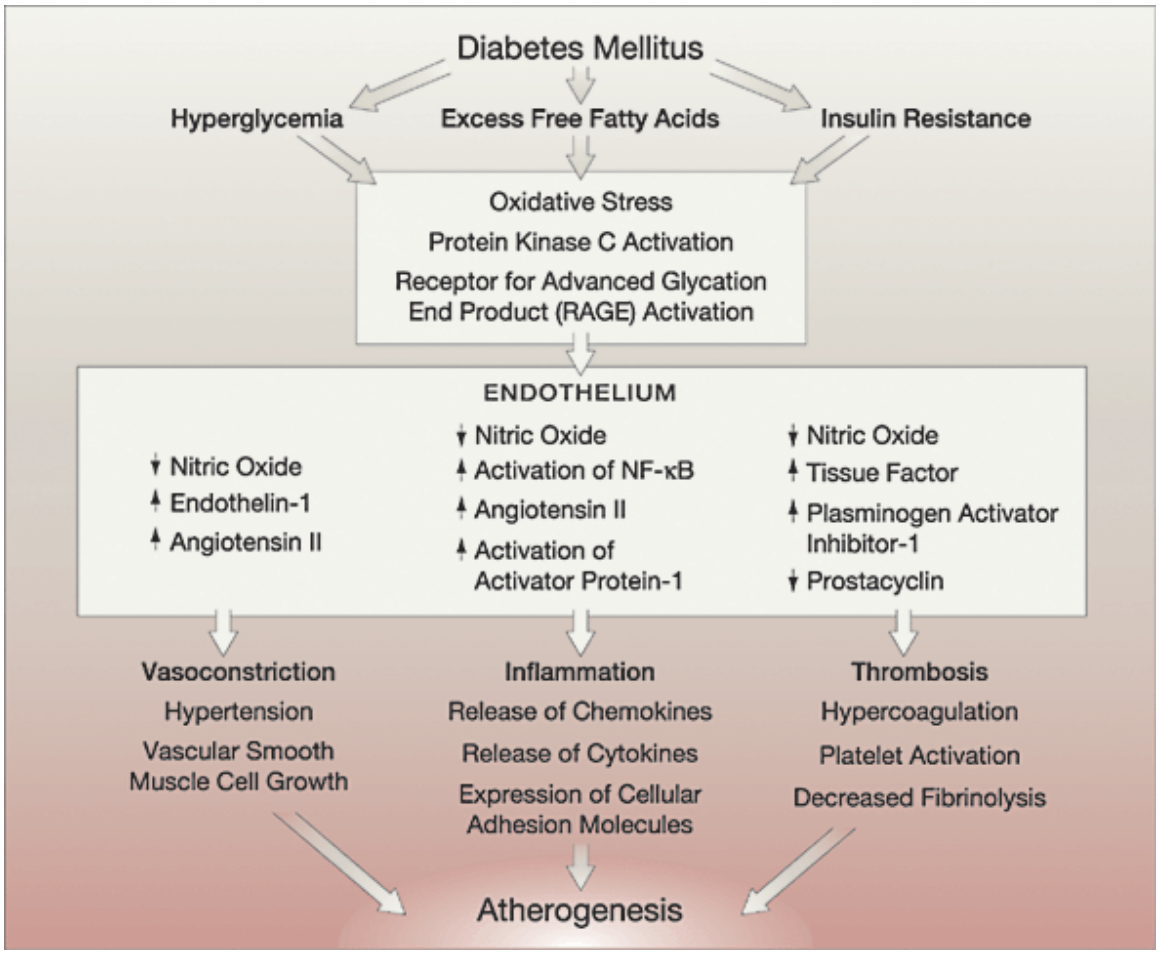

Figure 1.5: Summary of the effects of diabetes on atherogenesis [4]

1.4 Strategies for Vascular Tissue Engineering

In tissue engineering, there are two generalized approaches: top-down, in which a synthetic or biological material that acts as a template is seeded with cells that then reorganize themselves and the scaffold, and bottom-up, or self-assembly. The scaffold-based, top-down approach to tissue engineering follows the schema of isolating cells from a patient,

expanding and possibly manipulating those cells *in vitro*, seeding those cells onto a scaffold, conditioning the scaffolds in a bioreactor, then implanting the new tissue engineered construct into the patient.[36]

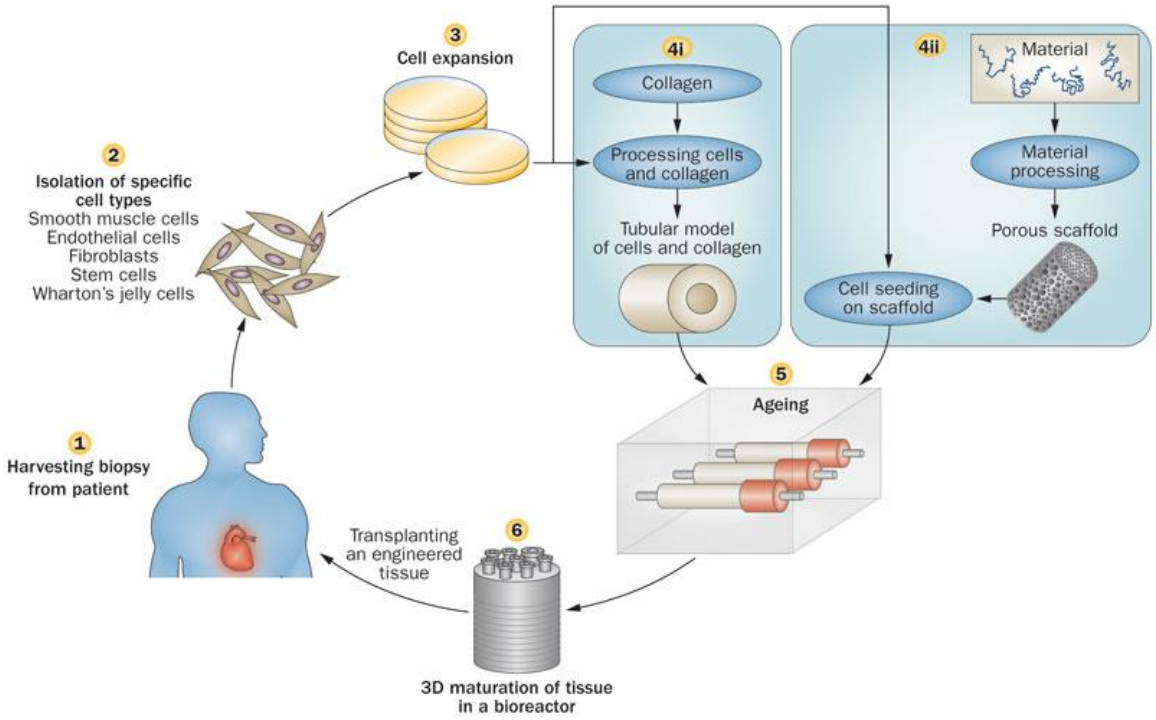

Figure 1.6: Scaffold-Based Approach to Tissue Engineering. [36]

1.4.1 Decellularized Tissue as a Biological Scaffold

The extracellular matrix (ECM) provides an ideal scaffold for tissue engineering.[3] Decellularized tissues maintain similar architecture, mechanical properties, and bioactivity to native tissues. This allows for cell in-growth, matched tissue compliance, and proper cell signaling, respectively.[32] Further, the use of fully decellularized xenogeneic tissue takes advantage of the readily-available source of tissues from slaughtered animals while

providing a scaffold that is composed of only extracellular matrix proteins, which are highly conserved in evolution, and thus do not elicit and immune response.[32] There is however, a careful balance to be achieved when using decellularized tissues as scaffolds: complete removal of immunogenic antigens and integrity of the ECM.[3,32,36]

There are a variety of techniques to decellularize tissues. These techniques vary based on the decellularization agents employed, physical methods of decellularization, and the manner in which the decellularization agents are applied.[10] Decellularization agents include hypertonic and hypotonic solutions, acid and bases, detergents, enzymes, and chelating agents.[10] Physical parameters include temperature, force (such as agitation or sonication), pressure and pressure gradients across the tissue, electric current and electroporation, perfusion of tissues, and use of supercritical fluids.[10] Decellularization techniques used in this project will be reviewed.

Water is the most readily available method for inducing hypotonic shock in cells. The lack of salts outside of the cell causes a massive influx of water into the cell due to osmotic imbalance, causing cells to lyse. However, this technique poorly removes cell debris after lysis.[10] Acidic and basic solutions increase solubility of cell cytoplasmic components, as well as aid in denaturation of proteins and degradation of nucleic acids; however acids and bases similarly catalyze the degradation of collagen and collagen crosslinks and glycosaminoglycans in the extracellular matrix.[10] This leads to poorer mechanical strength in tissues decellularized by strong bases.[10] Peracetic acid acts with a dual mechanism of

decellularization by removal of residual nucleic acids and sterilizing the decellularized tissue.[10]

1.4.2 Polyphenol Stabilization of Decellularized Tissue Scaffolds

Pentagalloyl glucose (PGG) is a polyphenol comprised of a central glucose moiety linked to five gallic acid units (**Figure 1.7**).[9,44] PGG has been shown to exhibit a variety of beneficial effects. First, PGG has a high affinity for proline-rich proteins, and PGG-bound elastin and collagen have been shown to resist enzymatic degradation.[14,38] PGG is an antioxidant and can act as a free radical sink.[1] PGG has also been shown to be anti-inflammatory by inhibiting cytokines such as TNFα and IL-6, possibly through inactivation of the transcription factor NFκB.[44]

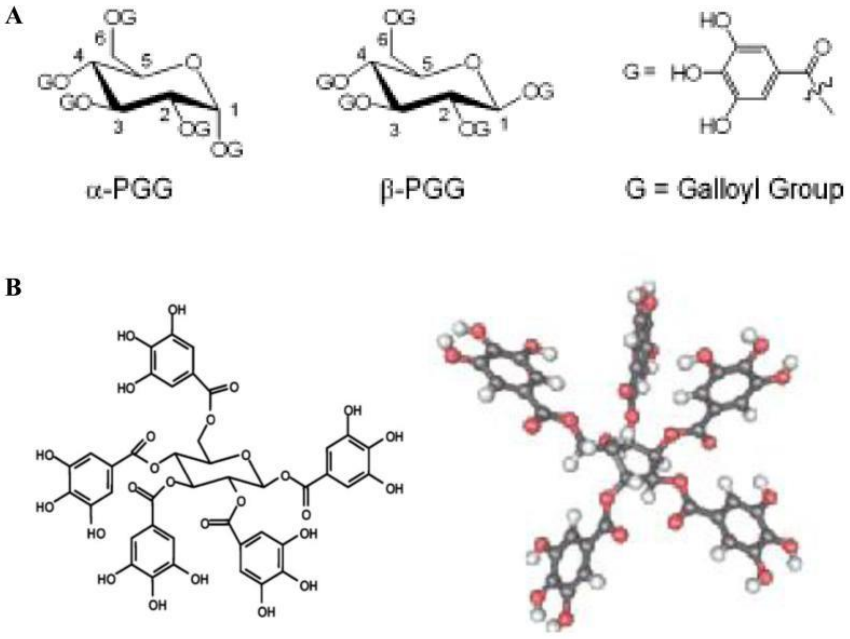

Figure 1.7: Steric Configurations and 3D structure of Pentagalloyl Glucose. [44]

Previously, PGG has been shown to mitigate the effects of diabetic damage on decellularized arterial and valvular scaffolds by reducing the accumulation of AGEs, reducing matrix calcification, and decreased inflammatory response of PGG-treated scaffolds when implanted in streptozotocin-induced type I diabetic rats compared to normal rats.[9]

1.4.3 Cell Sources for Tissue Engineered Vascular Grafts

Cells of the native vasculature consist of endothelial cells, smooth muscle cells, and fibroblasts. Efforts to seed decellularized grafts are centered on reconstituting these cell populations. While useful for research purposes, there are many drawbacks to using autologous primary vascular cells. Above all, isolation requires blood vessel biopsy, which adds additional complication, time, and possibly lack of availability in patients requiring revascularization surgery.[32] As an alternative to vascular cells, progenitor, adult stem cells from bone marrow or adipose, embryonic stem cells, or induced pluripotent stem cells are all under exploration.[32]

Of particular interest are adipose-derived stem cells (ADSCs), a multipotent cell population capable of differentiating into a variety of cell types, including each of the cell types in the blood vessel wall.[6,12] Compared to other sources of adult stem cells, ADSCs are easily isolated in large quantities with minimally invasive biopsy.[6] ADSCs and other mesenchymal stem cells (MSCs) have garnered attention for their immunomodulatory

phenotype.[16] ADSCs and MSCs are able to suppress inflammation in part by suppressing activation and proliferation of immune cells.[23]

1.4.4 Mechanical Conditioning

One of the weaknesses of modern cell biology is the reliance on static cell culture on tissue culture plastic. While is provides a convenient way to expand and study cells, it is a wholly unrealistic method for replicating *in vivo* processes. To greater increase understanding of basic cell biology, and to bridge the gap between the bench and the bedside, improved cell culture techniques are needed, and bioreactors offer a method to do so.

Native vasculature experiences circumferential stretch from blood pulsation and shear stresses from blood flow. It has been shown that those forces effect smooth muscle cell and endothelial cell biology, as well as the differentiation of adipose-derived stem cells toward those lineages.[15,17] Further, bioreactors provide a method for even seeding of scaffolds, increase tissue oxygenation, and remove waste from cells more readily.

CHAPTER TWO: PROJECT MOTIVATION, SPECIFIC AIMS, AND SIGNIFICANCE

Current therapeutic approaches for treatment of small-diameter vascular diseases, such as PCI and CABG, offer significant improvements in patient health and lifespan, but require continuous anti-coagulation therapies and present the risk of subsequent risk of restenosis or other cardiovascular events, particularly in diabetic patients. Tissue engineering promises to address these needs, but most approaches fail to address the most common co-morbidities and pathologies in the patients in need of those technologies. To address both of these needs, a tissue engineered vascular graft is being developed that can withstand damage in a diabetic environment.

The overall goal of this project is 1) assess the effect of hyperglycemia on adipose-derived stem cells differentiated toward an endothelial phenotype by measuring metabolic and inflammatory markers for diabetes and 2) perform a feasibility study for the conditioning of cell-seeded decellularized porcine renal arteries in a vascular bioreactor. In the long term, these seeded scaffolds will be implanted *in situ* in the abdominal aorta of healthy and diabetic rats, and this project will contribute to the *in vitro* develop of the grafts.

Aim I: To develop a decellularized and polyphenol-stabilized porcine renal artery scaffold

Porcine renal artery segments were isolated by dissection of kidneys sourced from a local abattoir, decellularized using a previously validated protocol[13], then treated with

pentagalloyl glucose, a polyphenol previously shown to increase scaffold resistance to diabetic conditions[9]. Efficacy of decellularization was assessed by histological analysis and DNA content.

Aim II: To assess the in vitro resistance of endothelial-differentiated adipose derived stem cells to diabetic conditions

Human Adipose-Derived Stem Cells (hADSC) were differentiated for three weeks in an endothelial differentiation medium. hADSC and Human Aortic Endothelial Cells (hAEC) were cultured for one week in normal or high glucose media. Differentiation of hADSC was assessed by immunofluorescence, and protein expression of diabetic markers was assessed by Western Blot and Cytokine Array.

Aim III: To reseed decellularized scaffolds, condition in a vascular bioreactor, and assess resistance to diabetic conditions

Decellularized arterial scaffolds were dynamically seeded in a vascular seeding chamber or statically-seeded by pipetting with hAEC on the luminal surface and Human Aortic Adventitial Fibroblasts (hAAFb) on the adventitial surface, then conditioned in a vascular bioreactor in normal or high glucose media for four weeks. Cellularity of the TEVG was assessed by Live/Dead Cell Viability Assay and Scanning Electron Microscopy.

CHAPTER THREE: PREPARATION AND CHARACTERIZATION OF DECELLULARIZED AND PENTAGALLOYL GLUCOSE-STABILIZED PORCINE RENAL ARTERY SCAFFOLDS

3.1 Approach and Rationale:

Decellularized xenogeneic tissues offer a readily available source of highly biocompatible and bioactive scaffolds that match the native architecture, biochemistry, and mechanical properties as native arteries. Porcine renal arteries have previously been demonstrated to provide a consistent source of small diameter arteries that could be re-seeded and implantation *in situ* in rat abdominal aortas for *in vivo* testing of a TEVG[14]. That decellularization technique was replicated, and this chapter shows that technique and the verification done on every round of scaffold preparation to demonstrate complete decellularization.

3.2 Materials and Methods:

3.2.1 Scaffold Preparation

Kidneys were collected from a local abbatoir (Snow Creek Meat Processing, Seneca, SC) and transported on ice until further processing. Excess adipose tissue was trimmed off and the renal artery of each kidney was identified. The arteries were clamped and adherent extravascular tissue was removed by blunt dissection until the tertiary branches of the renal artery were exposed. The arteries were then cut to select pieces that were 1-3 mm inner diameter, ≥1.5 cm in length, and free of holes or small branching arteries or arterioles. At this stage, some fresh artery pieces were collected and transferred to 10% phosphate-

buffered formalin (Fisher Scientific) for histological analysis or frozen and stored at -80°C to await digestion and isolation of DNA.

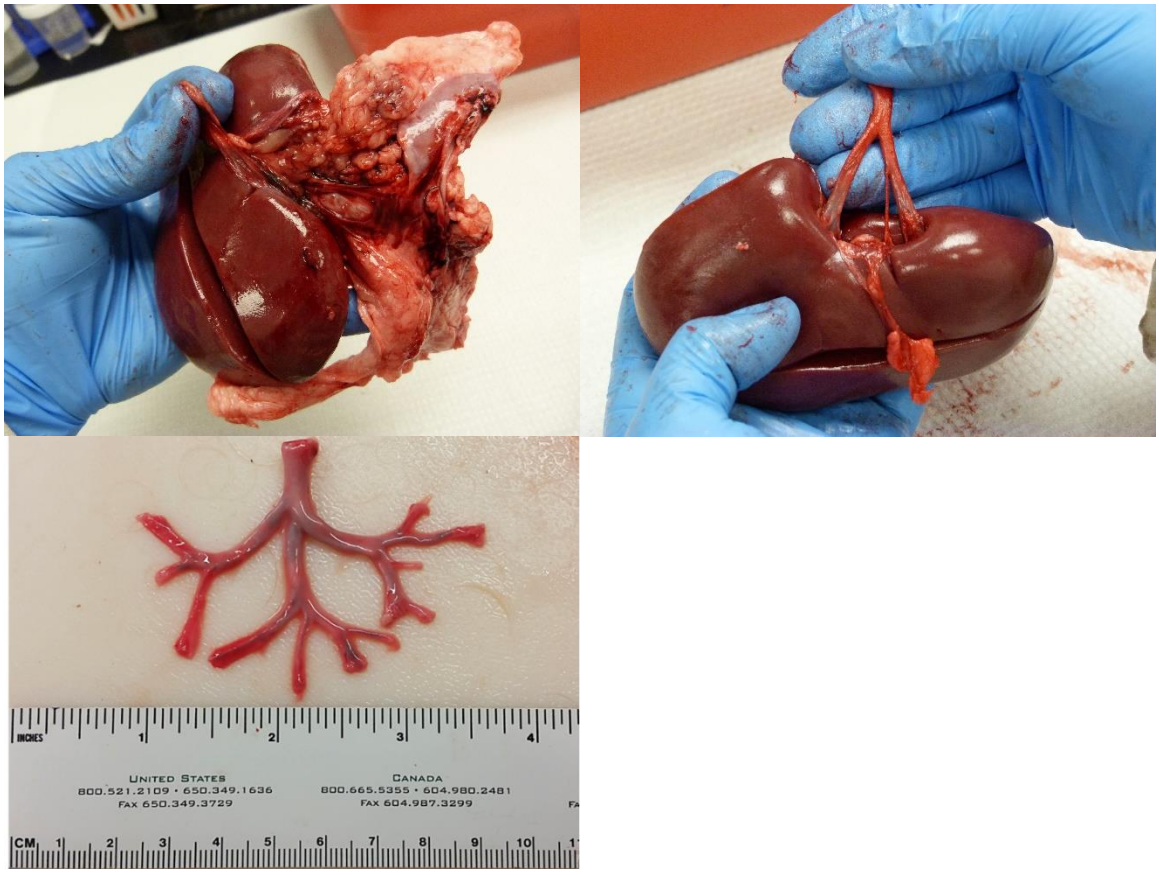

Figure 3.1: Dissection Process for Porcine Kidneys. Extrarenal connective tissue (**A**) was first removed. The primary renal artery is isolated (**B**), then non-vascular tissue is removed. This is done by grasping extravascular tissue, which is loosely attached to the artery adventitia, and pulling it away from the artery. Large pieces of extravascular tissue, kidney tissue, and adipose tissue are trimmed with scissors. Once renal artery branches too small for use (those with an inner diameter <1 mm or length <1 cm) are exposed, the entire hierarchical structure is trimmed off. Individual portions are measured to select for the most optimal scaffold pieces (**C**), those with inner diameter 1-2 mm and length >1.5 cm, and then cut away from the rest of the branches.

3.2.2 Decellularization of Porcine Renal Arteries

The selected fresh arteries were then immersed in distilled and deionized water (ddH_2O) overnight at 4°C. This and al subsequent steps were performed at a ratio of 3 arteries per 100 mL of solution. Following overnight immersion in hypotonic solution, the artery pieces were transferred to 0.1 M NaOH (sodium hydroxide, Fisher Scientific) solution in ddH_2O and agitated on a shake plate at 37°C for 3 hours. The arteries were washed for 30 min each in several changes of ddH_2O at room temperature while shaking until the decanted wash solution reached pH<8. The arteries washed once with phosphate-buffered saline solution (PBS, Corning), then immersed in fresh PBS and stored again overnight at 4°C.

3.2.3 Sterilization and Stabilization of Decellularized Arteries:

Following overnight storage, the arteries were transferred to sterile containers and immersed in 0.22 μm-filtered 0.1 M peracetic acid (Sigma Aldrich) in PBS, pH =7.4, and shaken at room temperature for 2 hours in the dark. The arteries were then rinsed in 3 changes of sterile PBS for 30 min each.

The arteries were then washed in 0.22 μm-filtered 1M PGG (N.V. Ajinomoto OmniChem S.A.), 50 mM 4-(2-hydroxyethyl)-1-piperazineethanesulfonic acid (HEPES, Fisher Scientific), 8 mM sodium chloride (Fisher Scientific), 20% isopropanol (Acros Organics), in ddH_2O, pH=5.5, shaking, overnight at room temperature in the dark. The arteries were then rinsed, shaking, in three changes of PBS for 15 min each, one change for 2 hours, then

three changes for 15 min each. The arteries were then stored in sterile PBS with 1% Pen/Strep (10,000 IU/mL Penicillin, 10,000 μg/mL Streptomycin, Mediatech, Inc.) at 4°C for up to two months.

3.2.4 Histological Analysis

Upon completion of decellularization, arteries were immersed in 10% phosphate-buffered formalin at a ratio of greater than 100 mL formalin per cm^3 of tissue for 24 to 48 hours. Next, fresh and decellularized arteries were paraffin-embedded with a Tissue-Tek VIP Tissue Processor (Sakura Finetek USA, Inc.). Samples were embedded in paraffin blocks, cut into 5 μm-thickness sections, fixed onto histology slides (Premiere) and heated at 56°C overnight to fix the artery sections to the slides.

Slides were de-paraffinized in xylenes (Fisher Scientific), dehydrated in progressive alcohols, and hydrated to distilled water, then stained with 1) 4',6-diamidino-2-phenylindole (VectaShield Hard Set Mounting Medium with DAPI, Vector Labs, Inc.) for the presence of nuclei (figure), 2) hematoxylin and eosin for nuclei and extracellular matrix structure, or 3) Masson's Trichrome (Poly Scientific R&D Corp) for collagen, muscle, and nuclei.

3.2.5 Quantitative and Qualitative Assessment of DNA Content

To assess DNA content, fresh and decellularized arteries were first frozen and stored at -80°C, then lyophilized at -40°C and 0.01 mbar for 24 hours. Samples were weighed to

establish dry weight for DNA concentration comparison and to assure samples were <25 mg. DNA was isolated using a DNeasy Blood and Tissue® Kit (Qiagen) following the manufacturer's instructions for animal tissue extraction. DNA concentration was assessed by Quant-iT PicoGreen® dsDNA Assay Kit (Invitrogen) following the manufacturer's instructions. Samples and standards were assayed in triplicate.

A 1% agarose (BM Biomedicals, LLC) gel was prepared in 0.5X TBE Buffer (90 mM Tris(hydroxymethyl)aminomethane, EMD Chemicals, 90 mM Boric Acid, Fisher Scientific, and 1.6 mM Ethylenediaminetetracetic acid (EDTA), Sigma Aldrich, in ddH_2O, pH=8.3), microwaved until the agarose melted, then 1.3 μm Ethidium Bromide (Bio-Rad Laboratories) was added when the gel solution cooled to <60°C. The gel was poured into a Gel Caster (Bio-Rad Laboratories) with a 20-well comb for 30 min. Sample and blank (nuclease-free water, Acros Organics) dilutions were prepared in a 1:5 dilution in 6X Blue/Orange Loading Dye (Promega) and DNA standard (100 μg/mL 1kb DNA ladder, Promega) was prepared in a 1:6 dilution in loading dye. 20 μL ladder, blank, or sample were loaded per well. The gel was immersed in 1X TBE Buffer and run at 100V and 3 mA for 75 min. The gel was imaged in a ChemiDoc XRS+ Gel Imager (Bio-Rad Laboratories) according to the manufacturer's instructions.

3.3 Results and Discussion

3.3.1 Gross Analysis

Color change in the scaffolds was notable between fresh and decellularized arteries. Immediately after dissection, arteries appeared a light red, but not quite pink. Following overnight immersion in water, the arteries were mostly white with a pink tinge. Following NaOH treatment, the arteries appeared pale white with a yellow tinge and are slightly translucent. Following peracetic acid treatment, the arteries appeared pale, opaque white.

3.3.2 Histological Analysis

Adequate decellularization of porcine renal arteries was first assessed by the absence of cells or cell nuclei and by the preservation of extracellular matrix proteins and morphology. DAPI binds strongly to nucleic acids, and thus can be used to visualize nuclei location and shape. It is often used as a counterstain against other fluorescent staining techniques. In this context, it provides a quick and simple method for visually detecting the presence of nuclei and their location. The use of this technique becomes particularly useful when examining tissues that appear decellularized by gross analysis, but histology or DNA extraction show that decellularization was not complete. In such tissues, nuclei may appear diffuse, indicating cells and nuclei have lysed but not adequately removed, or may only appear in the middle of a layer of tissue, indicating that decellularization agents insufficiently penetrated the tissue. Staining was compared against freshly dissected arteries that were rinsed lightly in PBS to remove adhering clots, then immediately fixed in formalin, then paraffin-embedded following 24 hours.

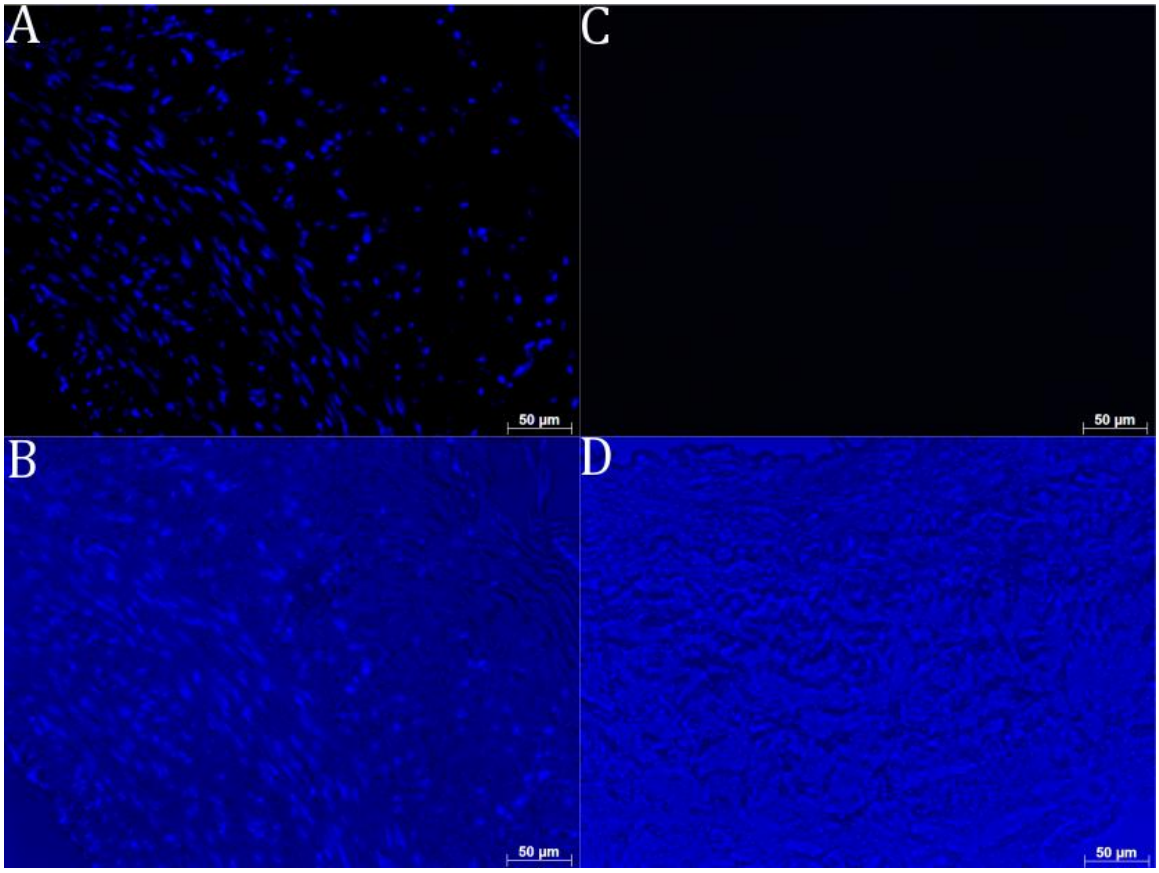

Figure 3.2: DAPI staining of fresh and decellularized arteries. Fresh arteries show abundant cellularity in the intimal, medial, and adventitial layers of the arteries (**A** and **B**). Decellularized arteries show a total lack of cellularity in all three layers. (**C** and **D**). Images were acquired under a blue filter (**A** and **C**). To show placement of cells with respect to tissue structure, bright light was added in addition to a blue filter (**B** and **D**). All images taken at 200X magnification.

Histological analysis indicates full removal of cells in the decellularized arteries. DAPI staining (figure) demonstrates a total lack of cells in any layer of the tissue. In fact, it is not possible to see any tissue on the slide without white light (figure). Hematoxylin and Eosin staining demonstrate that 1) cells were removed and 2) the architecture of the extracellular matrix remained intact, as evidenced by the "holes" in which cells would have resided.

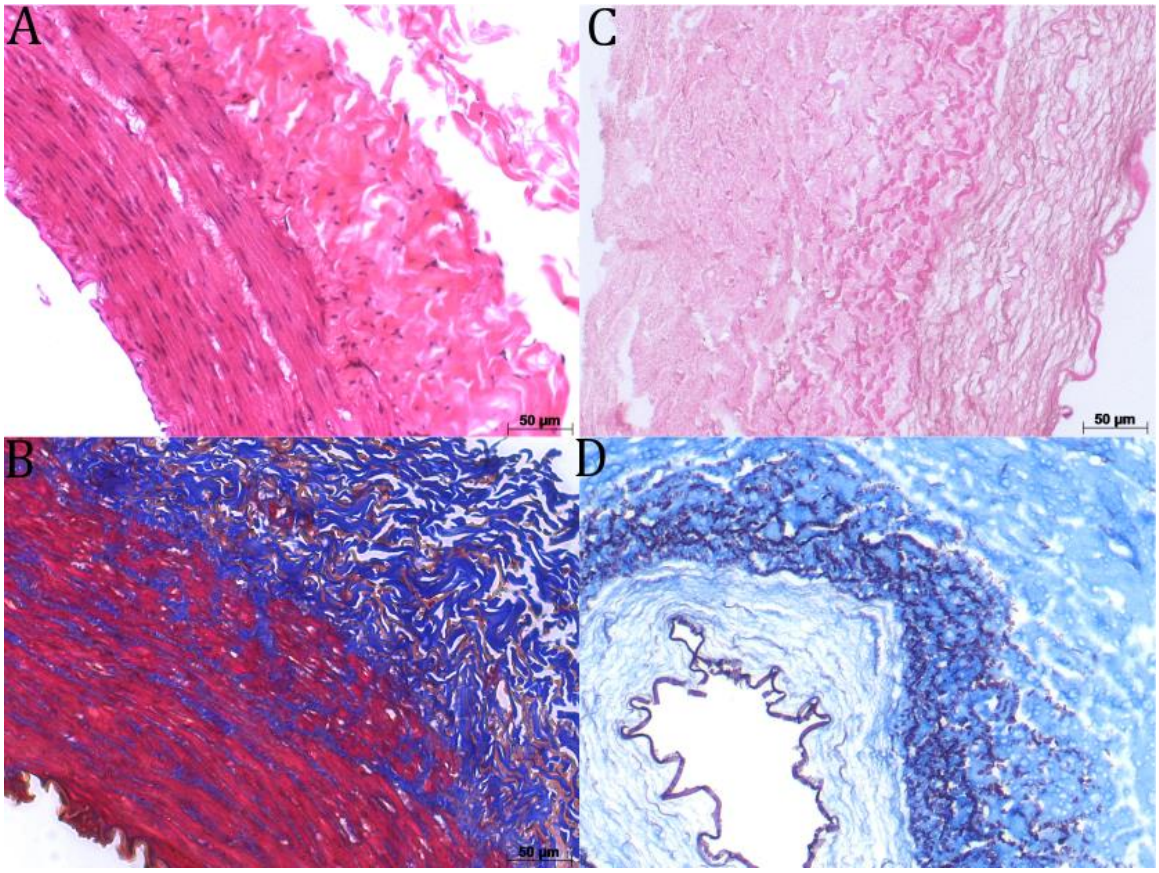

Figure 3.3: H&E and Masson's Trichrome staining of fresh and decellularized tissue. Hematoxylin is a dark blue to violet basic stain that binds to negatively charged structures, such as nucleic acids, and eosin is a pink to red acidic stain that binds to positively charged structures, such as proteins. The more concentrated the protein concentration, the stronger eosin staining appears, and thus ECM proteins in isolation appear light pink and intact cells appear darker pink to red. Masson's Trichrome is a three-colored stain that stains collagen blue, muscle red, and nuclei dark red to black. Fresh arteries (**A** and **B**) demonstrate intact endothelium, densely populated medial layers, and loose, collagen-heavy adventitia. Decellularized arteries show a lack of stained nuclei and white spaces where cell have been removed (**C**) and show removal of smooth muscle cells from all layers of the tunica media (**D**). Additionally, decellularized arteries demonstrate retention of the ultrastructure of the tissue. **A**, **B**, and **C** were taken at 200X magnification. **D** was imaged at 100X magnification.

3.3.3 DNA Content

Analysis of DNA content indicates sufficient removal of immunogenic cellular material. DNA content has become established in the use of decellularized organs as scaffolds for tissue engineering, as DNA itself is highly immunogenic and it can also serve as a proxy for the presence of other potentially immunogenic materials in the ECM (Badylak, 2011). Generally, a tissue can be considered to be non-immunogenic if the decellularized organ meets the following criteria: 1) contains less than 50 ng of DNA per mg of tissue (dry weight), 2) any residual DNA is less than 300 base pairs in length, and 3) lack visible nuclear material by conventional histological analysis, namely DAPI and hematoxylin and eosin (Badylak, 2011). In these scaffolds, a 94.3% reduction of DNA concentration was achieved, and the concentration was significantly level less than the threshold level of 50 ng DNA/mg tissue dry weight. Further, gel electrophoresis with ethidium bromide staining failed to show any visible sign of DNA content in the decellularized tissue.

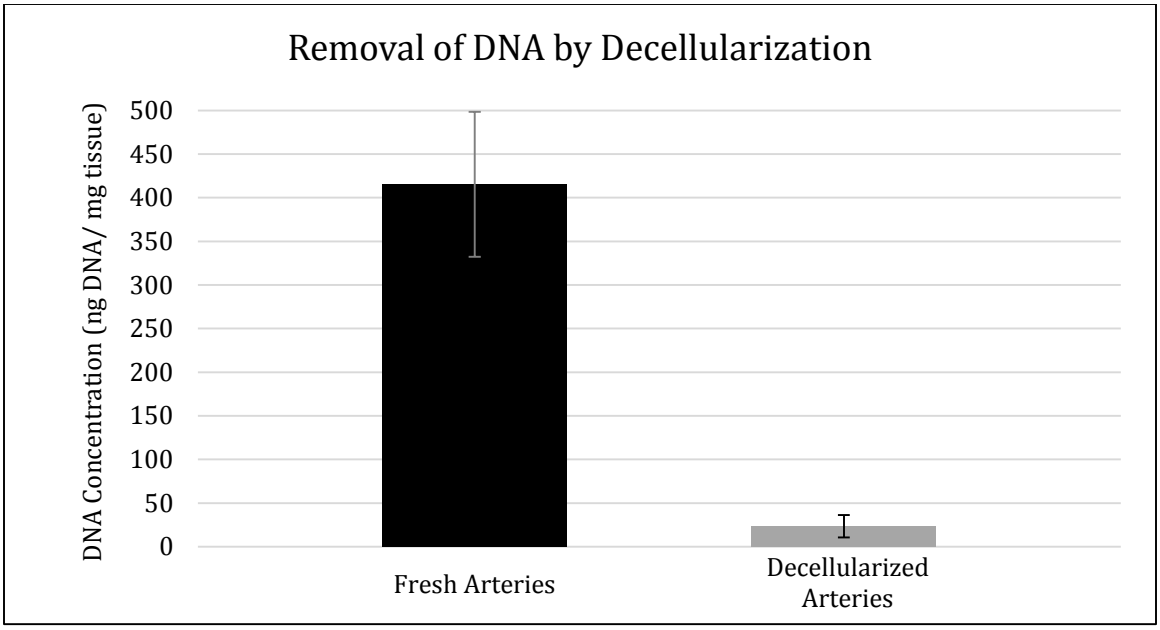

Figure 3.4: Quantification of DNA isolated from fresh and decellularized arteries. The concentration of DNA isolate from fresh and decellularized arteries was determined by Picogreen® Assay. The total mass of DNA in each sample was calculated from the assayed concentration and compared to the dry weight after lyophilization of the sample tissue.

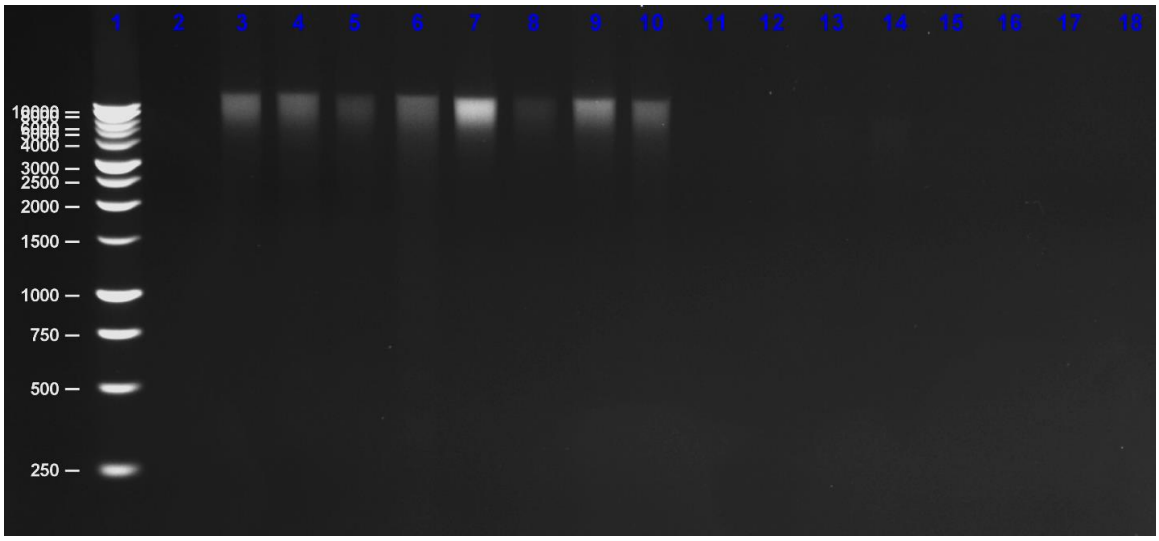

Figure 3.5: Agarose gel electrophoresis on DNA isolated from fresh and decellularized arteries. Lane

1 is a Promega 1 kb DNA Ladder. Lane 2 is a blank. Lanes 3-10 are DNA isolated from fresh porcine renal artery branches. Lanes 11 through 18 are DNA isolated from decellularized porcine renal arteries. The molecular weight guide is measured against the ladder and is units of base pairs.

3.5 Conclusions:

Previous use of this technique showed by immunostaining that α-galactosidase, a powerful porcine immunogen, was removed upon decellularization, subsequent cytocompatibility testing demonstrated safety of these grafts[14]]. Removal of cells was demonstrated in tandem by histological analysis that showed a total lack of cells and by 94.3% reduction in DNA content of the scaffolds. Taken with previous validation studies, these arteries should not elicit an immune response in *in vitro* re-seeding experiments (Chapter 5) or in animal model testing.

CHAPTER FOUR: ASSESSING DIFFERENTIATION AND *IN VITRO* DIABETES RESISTANCE OF ADIPOSE-DERIVED STEM CELL-DERIVED ENDOTHELIAL CELLS

4.1 Approach and Rationale:

Arguably the most important cell for generating a tissue engineered vascular graft because a confluent layer of endothelial cells is currently the only known truly non-thrombogenic surface.[8] However, endothelial cells are particularly prone to diabetic complications because of their inability to control intracellular glucose flux during hyperglycemia[30] and thus will likely be prone to contribute to failure of a TEVG if implanted in a diabetic patient. To control inflammation and modulate the immune response, adipose derived stem cells differentiated toward and endothelial fate offer a promising choice. To assess the resistance of differentiated ADSCs to diabetic conditions, ADSCs will be differentiated, then cultured in normal or high glucose media. Markers for endothelial differentiation, metabolic pathway markers (mTOR and PPARγ), oxidative stress (NOX1), and inflammation (NFκB, TNFα, IFNγ, and IL12) were analyzed to determine the diabetes resistance potential of differentiated ADSCs compared to endothelial cells.

4.2 Materials and Methods:

4.2.1 hADSC and hAEC Culture

Human adipose-derived stem cells (hADSC p3, Invitrogen) were plated at 5,000 cells/cm^2 in MesenPRO RS^{TM} Medium (Life Technologies) and cultured at 37°C and 5% CO_2.

MesenPRO RS™ Medium was prepared from MesenPRO RS™ Basal Medium (Life Technologies) with 2% MesenPRO RS™ Growth Supplement (Life Technologies), 2 mM L-glutamine (Life Technologies), and 1% Pen/Strep. Media was changed 24 hours following plating and every 48 hours subsequently. hADSCs were subcultured at 80% sub-confluence, approximately every 3 days. At passage 6, hADSCs were plated at 3,500 cells/cm^2 in endothelial differentiation medium and cultured for 21 days with media changes every 3 days. Endothelial differentiation medium was prepared as follows: Dulbecco's Modified Eagle Medium (DMEM) with sodium pyruvate, L-glutamine, and 1 g/L glucose (Corning) with 2% Fetal Bovine Serum (FBS, Atlanta Biologicals), 1% Pen/Strep, 0.5 ng/mL VEGF, and 20 ng/mL Insulin-like Growth Factor 1 IGF-1.

Human Aortic Endothelial Cells (hAEC p4, Lonza) were plated at 5,000 cells/cm^2 in Endothelial Growth Medium 2 (EGM™-2, Lonza) and cultured at 37°C and 5% CO_2. EGM™-2 was prepared from Endothelial Basal Medium (EBM™-2, Lonza) and EGM™-2 SingleQuots Kit (Lonza). Media was changed 24 hours following plating and hAEC were subcultured at 90% sub-confluence, approximately every 4 days.

At passage 6, hADSC-derived endothelial cells (hADSC-EC) and hAEC were passaged and plated onto well plates in normal or high glucose media at 3,500 cells/cm^2. Normal media was prepared from DMEM with 2% FBS and 1% Pen/Strep to yield 5.5 mM glucose and high glucose media was prepared from DMEM with 2% FBS, 1% Pen/Strep, and 4.5

g/L D-Glucose Monohydrate (EMD Chemicals) to yield 30 mM glucose. Cells were cultured for 1 week at 37°C with 5% CO_2 and media was changed daily.

4.2.2 Immunofluorescence

To assess differentiation of adipose-derived stem cells to an endothelial cells, hADSC-EC were stained with markers for endothelial cells: CD31, Von Willebrand Factor (vWF), and VEGFR2. First, media was removed and cells were fixed in 4% paraformaldehyde in PBS, pH=6.9 for 20 min, permeabilized with 0.3% Triton X-100 (Alfa-Aesar) in PBS for 10 min, then blocked with 5.0% Bovine Serum Albumin (BSA, Rockland, Inc.) and 0.5% Triton X-100 in PBS for 2 hours. Cells were incubated in primary antibody solution, diluted in diluted blocking solution (2.5% BSA, 0.25% Triton in PBS), overnight at 4°C slowly shaking: 10 μg/mL Rb Anti-CD31 IgG (Abcam ab28364), 20 μg/mL Rb Anti-vWF IgG (Abcam ab9378), or 1 μg/mL Rb Anti-VEGFR2 IgG (Abcam ab39638). Cells incubated in secondary antibody solution (4 μL/mL in diluted blocking solution, AlexaFluor 488 Do Anti-Rb IgG, Thermo Scientific) and counterstained for nuclei with 1.43 μM DAPI in PBS for 5 min at room temperature and in the dark. Cells were rinsed with PBS between each step. Cells were imaged using company.

4.2.3 Assessment of Protein Expression - Western Blot and Cytokine Array Panel

Cells were lysed by direct application of RIPA Buffer to the well plate and disruption with a cell scraper. RIPA Buffer was prepared from 50 mM Tris-HCl (EMD Chemicals), 150 mM Sodium Chloride (Fisher Scientific), 1 mM EDTA (Sigma Aldrich), 1% Triton X-100

(Alfa Aesar), 1% Sodium Deoxycholate (Fisher Scientific), 0.1 Sodium Dodecyl Sulfate (Avantor Performance Materials), and 0.1% Protease Inhibitor Cocktail (Sigma Aldrich P-8340) in ddH_2O, pH=7.4. Cell lysates were centrifuged at 12,000 xG for 15 min at 4°C and the supernatant transferred and stored at -20°C until use. Protein concentrations were assessed by Bicinchoninic Acid Assay (BCA Assay, Thermo Scientific) according to the manufacturer's directions using the plate method. Samples and standards were assayed in triplicate.

4.2.3.1 Western Blot

To prepare samples for electrophoresis, the volume of each sample necessary to yield 15 μg/lane was calculated. Samples were diluted in 1X non-reducing buffer (company) with concentration β-Mercaptoethanol (β-ME, company) and boiled 5 minutes to denature the proteins. Electrophoresis and transfer were run for 90 min at 100V each. The membranes were blocked overnight at 4°C in 2% nonfat dry milk (NFDM, Bio-Rad Laboratories) in Tris buffer, then blotted overnight at 4°C with 2.00 μg/mL Rb anti-mTOR (Abcam ab51089), 1.00 μg/mL Mo anti-PPARγ (Abcam ab41928), 0.500 μg/mL Rb anti-NOX1 (Abcam ab55831), or 0.621 μg/mL Rb anti-NFκB (Abcam ab32360) in diluted blocking solution. Primary antibody detection was achieved using a Mo/Rb secondary antibody and reagents from a BM Chemiluminescence Western Blotting Kit (Roche). The blots were imaged using a ChemiDoc XRS+ Gel Imager (Bio-Rad Laboratories) and analyzed by relative band intensity (densitometry) and molecular weight using the supplied software (ImageLab, Bio-Rad Laboratories).

4.2.3.2 Cytokine Array Panel

The relative expression of the cytokines TNFα, IL12, and IFNγ were assessed using a Human Cytokine Panel Array A by R&D Systems (Bio-Techne) following the manufacturer's directions with minor exceptions. Briefly, protein samples were obtained from cell lysates as described above. Four nitrocellulose membranes containing anti-cytokine antibodies printed in duplicate were blocked for 1 hour at room temperature. Samples were diluted to 100 µg protein in 1.5 mL supplied buffer, mixed with 15 µL antibody cocktail, and incubated 1 hour at room temperature. The blocking buffer was aspirated and each membrane was incubated in sample-antibody solution overnight at 4°C. The membranes were washed with water and dried, then rinsed in wash buffer. The membranes were incubated in Streptavidin-HRP solution for 30 min at room temperature, washed in wash buffer, dried, and developed in Chemi Reagent Mix. The membranes were imaged the same as for Western Blotting.

4.3 Results and Discussion

4.3.1 Differentiation of Adipose Derived Stem Cells

Differentiated hADSC showed positive immunofluorescence when stained with antibodies for CD31, VEGFR2, and vWF (**Figure 4.1A, 4.1B, and 4.1C**, respectively). The fluorescent brightness of differentiated hADSC was lower than that of hAEC stained for the same markers (**Figure 4.1**). Differentiated hADSC demonstrate a spindle-shaped

morphology unchanged from undifferentiated hADSC, whereas endothelial cells display a round, flattened morphology.

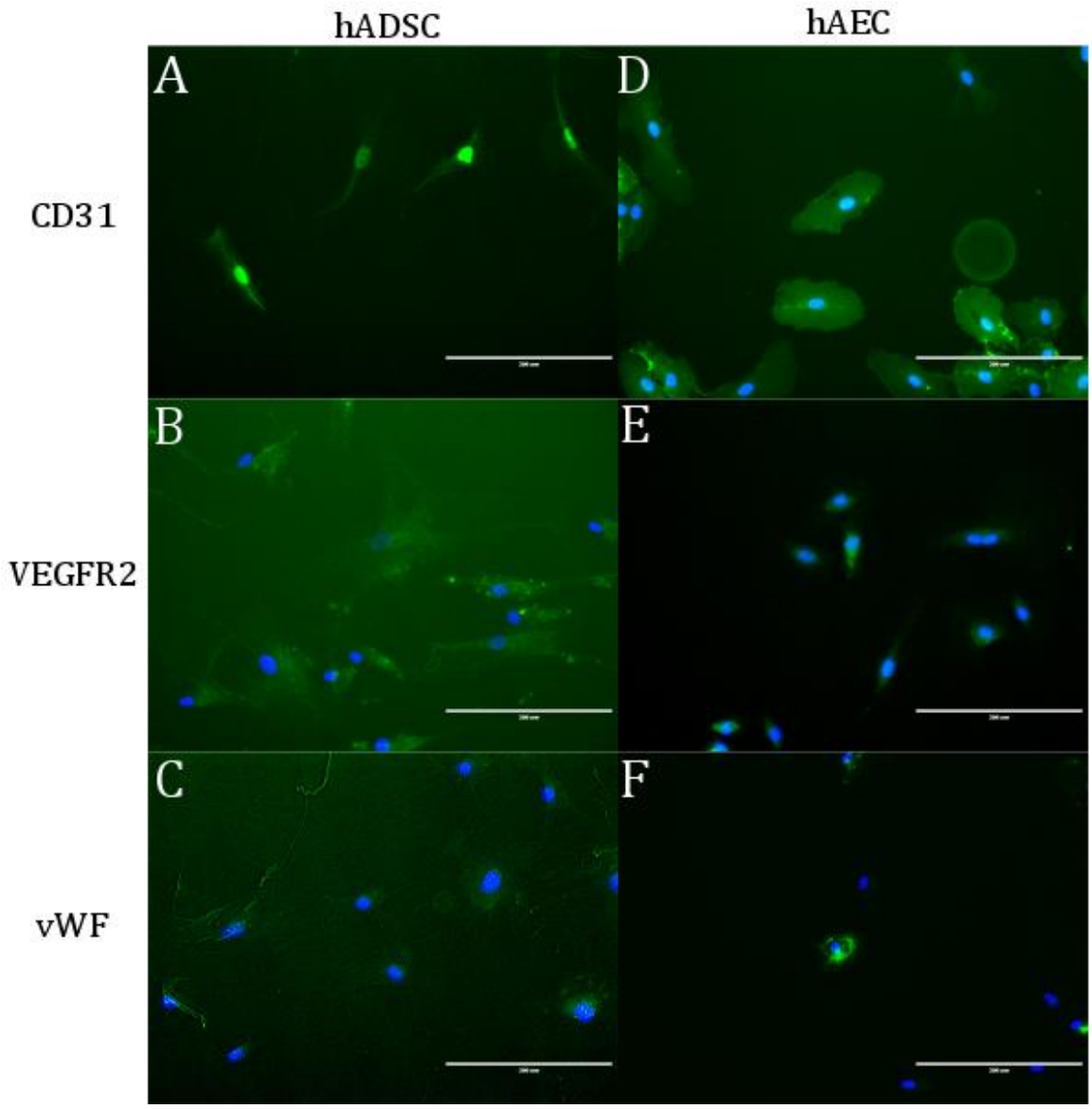

Figure 4.1: Immunofluorescent Staining of Differentiated hADSC and hAEC. Cells were stained for endothelial markers CD31 (**A** and **D**), VEGFR2 (**B** and **E**), and vWF (**C** and **F**). Images were taken at 200X magnification.

4.3.2 Analysis of Protein Expression

Both hAEC and differentiated hADSC show a trend toward increased mTOR expression in diabetic conditions compared to normal. Similarly, hAEC and differentiated hADSC show a trend toward increased NFκB in diabetic versus normal conditions, but was much greater for endothelial cells. Additionally, blots for NOX1 and PPARγ did not yield identifiable bands (**Figures A3** and **A4**). The experiment could not be performed again due to insufficient protein samples (see **Table A1** for protein yields and use in experiments).

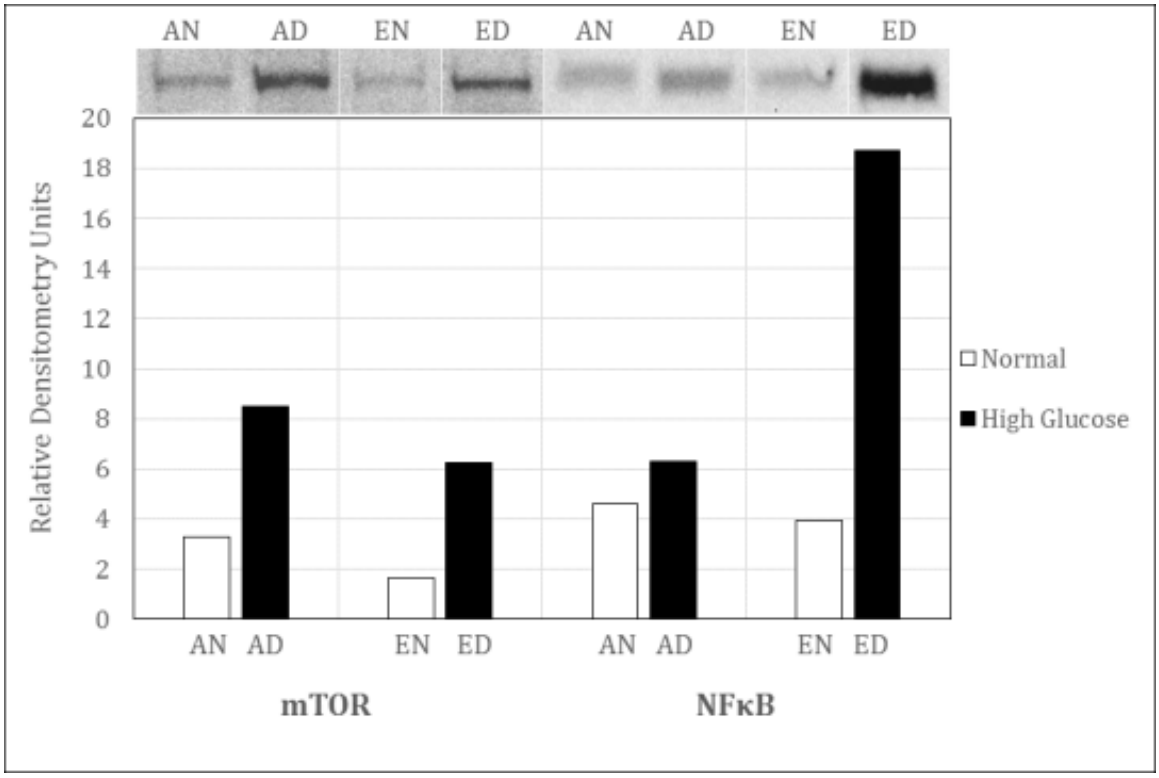

Figure 4.2: Analysis of Protein Expression in Differentiated hADSC and hAEC in Normal or High Glucose by Western Blot. AN = hADSC in normal media; AD = hADSC in high glucose media (diabetic); EN = hAEC in normal media; ED = hAEC in diabetic media; ADSC had a higher baseline expression of mTOR over hAEC (3.3 v. 1.6 Relative Densitometry Units, RDU) and had a greater fold-increase in expression in diabetic conditions (2.6-fold greater v. 3.8-fold). ADSC had a greater baseline expression of

NFκB (4.6 v. 3.9 RDU), but had a smaller fold-increase in expression in diabetic conditions (1.4-fold v. 4.7-fold). N=3, pooled, 15 μg protein per lane for all samples.

Cytokine expression analysis yielded mixed results. Most of the markers on the panel yielded no expression in any of the samples. This may be due to insufficient protein levels (see **Table A1**) or insufficient exposure to high glucose conditions to cause an inflammatory response. The markers that did show expression are shown in **Figure 4.3**. CCL2, CXCL1, and CXCL10 are chemokines that recruit inflammatory cells, particularly neutrophils and macrophages, to the site of inflammation. These markers are by ADSCs in high glucose conditions, CCL2 is also expressed in normal conditions. CD40 and ICAM-1 are a receptor for TNF and an adhesion molecule expressed on the cell surface for inflammatory cell attachment, respectively, and are expressed by differentiated ADSCs in high glucose. IL-18 and IL32α are activators of T cells and macrophages, respectively, and showed the greatest levels of expression in both differentiated ADSCs and hAECs in normal and high glucose. In differentiated ADSCs, the expression is increased in high glucose, but the trend is reversed in hAECs. Interleukins 4 and 10 are anti-inflammatory cytokines that promote M2 macrophage polarization and block the activation of NFκB, respectively. These are both expressed by differentiated ADSCs in both normal and high glucose conditions.

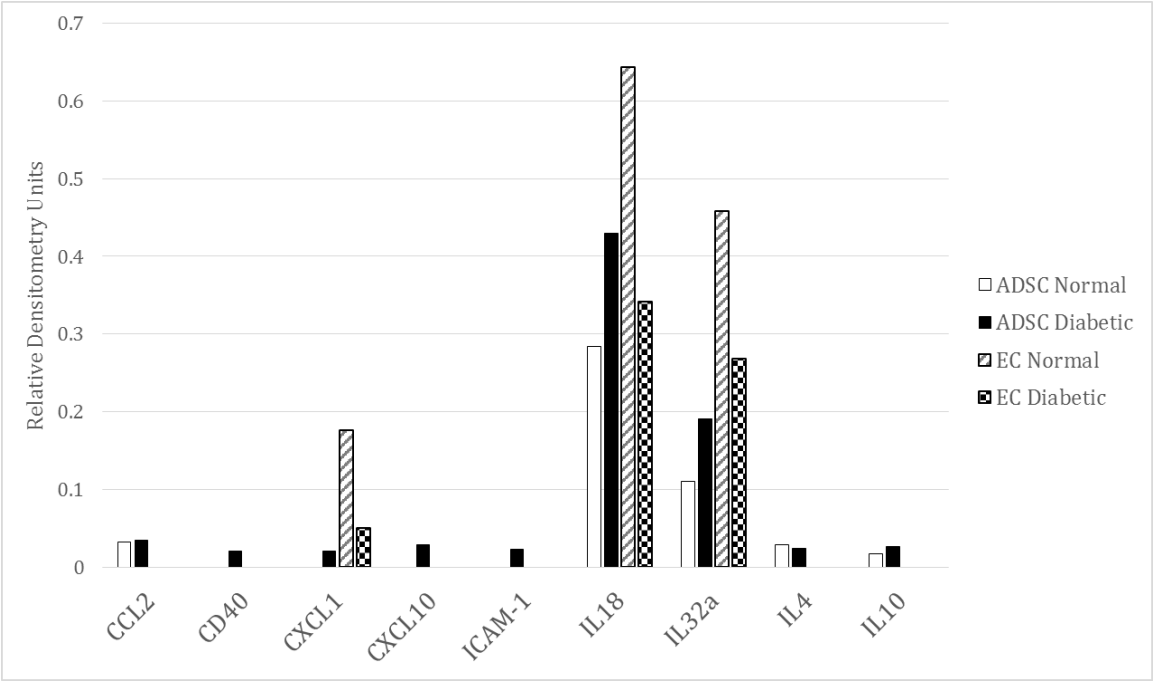

Figure 4.3: Analysis of Cytokine Expression in Differentiated sADSC and hAEC in Normal or High Glucose. CCL2 = Chemokine Ligand 2; CD40 = Tumor Necrosis Factor Receptor 5; CXCL1 = Chemokine Ligand 1; CXCL10 = Chemokine Ligand 10; ICAM-1 = Intracellular Adhesion Molecule 1; IL18 = Interleukin 18; IL32a = Interleukin 32a; IL4 = Interleukin 4; IL10 = Interleukin 10; N=3, pooled and 100 µg protein were used per membrane.

4.4 Conclusions

Endothelial-differentiated ADSCs showed differentiation toward an endothelial phenotype, but with some limitations. Immunofluorescence was weak in differentiated ADSCs, and cell morphology did not resemble endothelial cells. This confirms previous differentiation studies in ADSCs, which showed that full differentiation of ADSCs toward endothelium required shear conditioning in order for cells to uptake LDL or form tubules in hydrogels.[15] ADSCs demonstrated a similar response in altered expression of metabolic

markers and certain inflammatory markers to endothelial cells, but showed strong resistance to NFκB upregulation in diabetic conditions. Promisingly, differentiated ADSCs showed expression of interleukins 4 and 10, which shows promise that even after differentiation, these cells can modulate the phenotype of immune cells. In all, differentiated ADSCs demonstrate similar or improved resistance to inflammation or metabolic distress, depending on the marker, to endothelial cells in high glucose conditions. Although this did not support the hypothesis that differentiated ADSCs could mitigate the inflammatory response induced by high glucose conditions, this does show that ADSCs are a viable alternative to endothelial cells in vascular tissue engineering.

CHAPTER FIVE: RECELLULARIZATION AND BIOREACTOR CONDITIONING TO ASSESS *IN VITRO* RESISTANCE OF TISSUE ENGINEERED VASCULAR GRAFTS TO HIGH GLUCOSE TO HIGH GLUCOSE CONDITIONS

5.1 Approach and Rationale

In addition to 2D culture, to assess the *in vitro* diabetes-resistance of differentiated ADSCs, cell need to be conditioned and tested in an environment that mimics the *in vivo* environment. Shear stress has been shown to alter endothelial cell phenotype[8], and has been shown to be a requirement for full phenotypic differentiation of ADSCs[15]. This additional component should not only prepare TEVG for implantation, but should also provide data that corresponds more closely to eventual data from animal models. To accomplish this, a vascular bioreactor designed in the Biocompatibility and Tissue Regeneration Laboratory was used to condition the vessels. In addition, a vascular seeding chamber was used to dynamically seed cells onto decellularized and PGG-stabilized porcine renal artery scaffolds.

5.2 Materials and Methods

5.2.1 hAEC and hAAFb Culture

Human Aortic Endothelial Cells (hAEC p4, Lonza) were plated at 5,000 cells/cm^2 in Endothelial Growth Medium 2 (EGM^{TM}-2, Lonza) and cultured at 37°C and 5% CO_2. EGM^{TM}-2 was prepared from Endothelial Basal Medium (EBM^{TM}-2, Lonza) and EGM^{TM}-

2 SingleQuot Kit (Lonza). Media was changed 24 hours following plating and hAEC were subcultured at 90% sub-confluence, approximately every 4 days.

Human Aortic Adventitial Fibroblasts (hAAFb p2, Lonza) were plated at 3,500 cells/cm^2 in Stromal Cell Growth Medium (SCGM™, Lonza) and cultured at 37°C and 5% CO_2. SCGM™ was prepared from Stromal Cell Basal Medium (SCBM™, Lonza) and SCGM™ SingleQuot Kit (Lonza). Media was changed 24 hours following plating and hAAFb were subcultured at 80% sub-confluence, approximately every 4 days.

5.2.2 Dynamic Seeding of Decellularized Arterial Scaffolds

To neutralize any remaining PGG resident in the decellularized and PGG-stabilized scaffolds, scaffolds were immersed in a neutralizing solution of 50% DMEM and 50% FBS and incubated for 24 hours at 37°C. Scaffolds were then rinsed once with PBS. Arterial scaffolds were then cannulated by affixing each end of the scaffold onto 1/16" barbed quick-turn couplings and secured to the coupling with 6-0 sutures. Cannulated scaffolds were then stored in PBS + 1% Pen/Strep at 4°C until use (<24 hours).

Components of an in-house designed vascular seeding chamber (**Figure 5.1**) and parts to cannulate decellularized arterial scaffolds were individually cleaned, dried, packaged in sterilization pouches, and autoclaved. In a sterile environment set up in a laminar flow hood, the components were unpackaged and the chambers were partially assembled. 10/32"

x 1 1/2” bolts were fed through a rail, a silicone membrane, and the body of each seeding chamber. The Luer fitting were closed off using quick-turn plug caps.

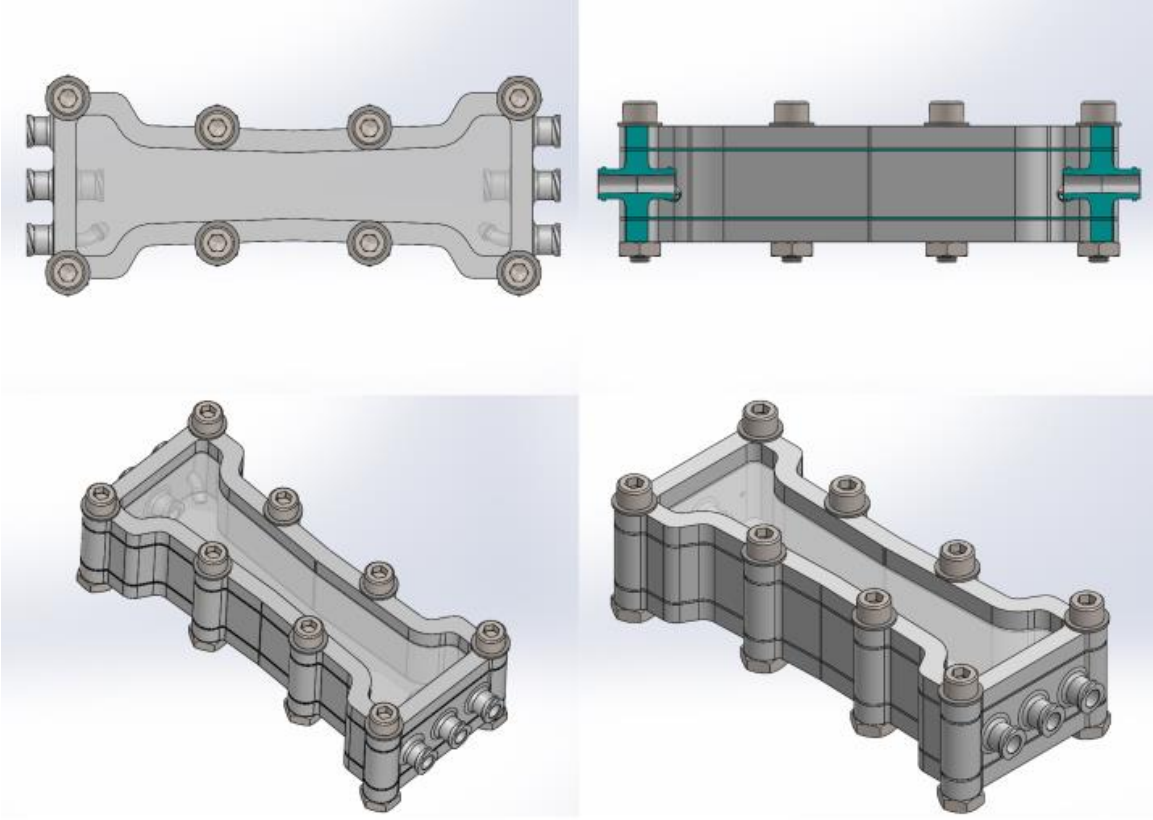

Figure 5.1: Solidworks Drawing of Vascular Seeding Chambers. Vascular scaffolds are fixed in the center of the chamber between the middle Luers. The left and right Luers can be used to seed the adventitia or to change media. All 6 ports are capped before removing the chamber from the sterile field. Silicone membranes on each side allow for gas exchange.

A fibroblast seeding solution was prepared by passaging hAAFb p6 and re-suspending at 50,000 cells/mL in DMEM + 10% FBS + 1% Pen/Strep. Two scaffolds were affixed to each seeding chamber and interconnected with 1/16” inner diameter tubing and quick-turn

barbed fittings. Seeding chamber assembly was then completed by addition of the bottom rail and nuts. To seed each pair of scaffolds with fibroblasts, one plug cap was removed from each side of a seeding chamber, and the chamber (on the adventitial side of the scaffolds) was flooded with ~50 mL fibroblast solution until air bubbles were removed. The plug caps were then placed back on the exposed Luer fittings on the seeding chambers.

The chambers were affixed to a rotary seeder controlled by a LabView program. The seeding chambers were rotated in 10 s intervals at 2 rpm (a 1/3 turn) for 8 hours. An endothelial cells medium was prepared from hAEC p6 in the same fashion as was the fibroblast solution. The lumen of the scaffolds were flooded with ~ l mL of endothelial solution, and the scaffolds were placed back on the rotary seeder overnight.

5.2.3 Bioreactor Setup

Components of an in-house designed vascular bioreactor (**Figure 5.2**) were cleaned, dried, packaged in sterilization pouches, and autoclaved or ethylene oxide sterilized. In a sterile environment, the components were unpackaged and the bioreactor was partially assembled by assembling all of the components except for the lid. The rotary-seeded scaffolds were removed from the sterile seeding chambers, transferred to the bioreactor chamber, and fitted to the quick fittings via 1/16" tubing and barbed quick-turn couplings (**Figure 5.3**). Five seeded scaffolds were placed in each bioreactor. The chamber was filled with ~500 mL normal or high glucose media (DMEM + 10% FBS + 1% Pen/Strep with 1 g/L glucose or DMEM + 10% FBS + 1% Pen/Strep with 5.5 g/L glucose, respectively) and the lid was

secured. The media reservoirs were filled with additional media (~1000 mL) and the caps were secured. The bioreactor was transferred to an incubator and affixed to a peristaltic pump. The pump was set to 50 mL/min and the incubator was at 37°C and 5% CO_2 (**Figure 5.4**). The flow rate was increased by 50 mL/min every 12 hours until the final flow rate was 250 mL/min. Seeded scaffolds were conditioned for 4 weeks, with one change media at 2 weeks.

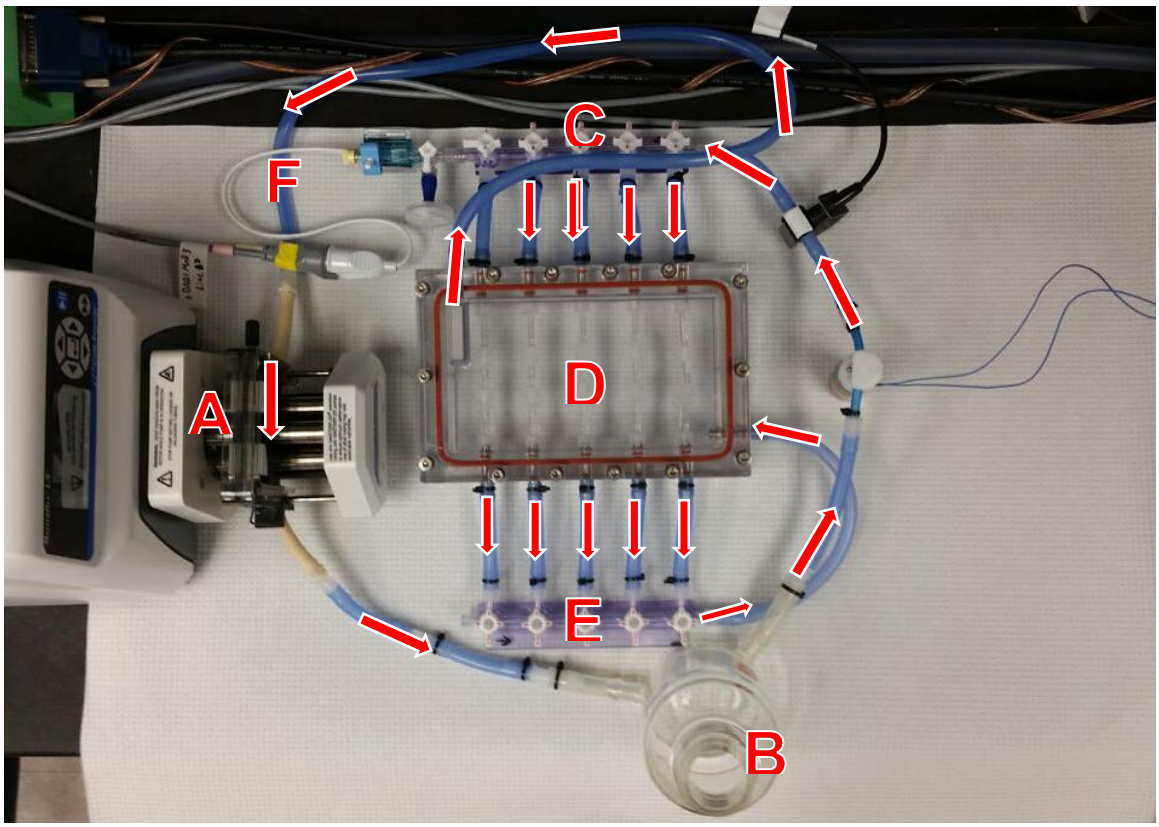

Figure 2.2: The Vascular Bioreactor. Flow originates from a pulsatile pump (**A**) that generates flow by rolling a metal bar across the tubing. The media flows through a media reservoir with a filter cap that allows for oxygen exchange (**B**). A manifold (**C**) splits the current evenly into 5 flow streams to flow through the lumen of each arterial scaffold (**D**), then re-converges them in a second manifold (**E**). The flow then passes

through the main chamber of the bioreactor to perfuse to the adventitia of the scaffolds and out the top. A second media reservoir (**F**, not shown) holds additional media and acts as a compliance chamber that dampens the pulsation generated by the pump.

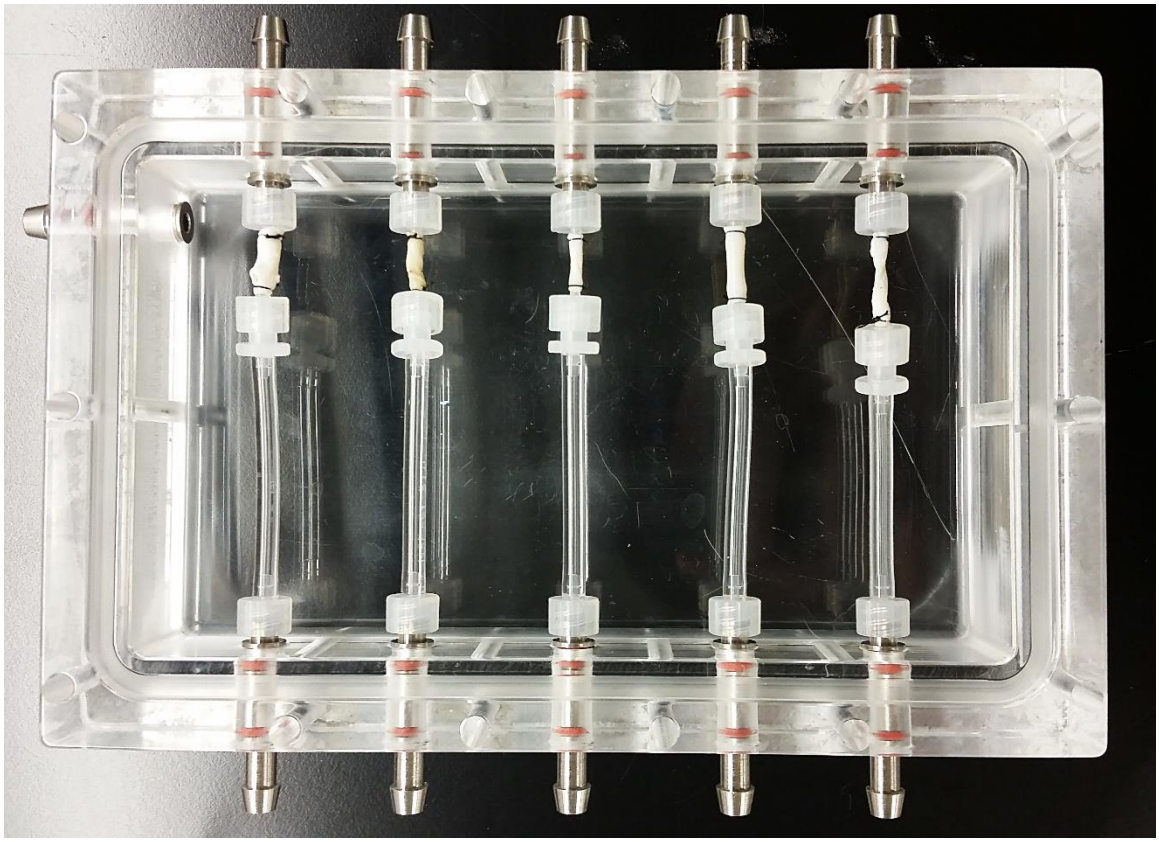

Figure 5.3: Cannulated Decellularized Arterial Scaffolds in the Vascular Bioreactor. The vascular bioreactor was first designed for the conditioning of re-seeded decellularized bovine carotid and mammary arteries, which have internal diameters of 5-6 mm and total length of ~9 cm. The vascular bioreactor was adapted using a smaller barbed quick-turn coupling and tubing to accommodate for the length.

Figure 5.4: Normal and High Glucose Vascular Bioreactors in an Incubator Just Prior to Removal

5.2.4 Assessment of Dynamically-Seeded TEVG Cellularity Following Bioreactor Conditioning

Upon removal from the bioreactor, two TEVG from each bioreactor were cut in half and each half was snap-frozen in liquid nitrogen and stored at -80°C. Three TEVG from each bioreactor had a 1 mm-long piece cut off for assessing cellularity via Lead/Dead Cell Viability Assay (Invitrogen). Briefly, TEVG pieces were immersed in Live/Dead working reagent prepared per the manufacturer's instructions for 35 min at room temperature and imaged under red and green filters at 100X magnification. The remainder of the TEVGs

left were cut in half. One half from each was immersed in 10% formalin for histological analysis, prepared as in *3.2.4* and the other half was fixed in Karnovsky's Fixative for 24 hours for scanning electron microscopy (SEM). Karnovsky's Fixative was prepared by dissolving 0.1M Cacodylic Acid (Omni Pur), adjusting the pH to 7.4, then adding 2.5% Glutaraldehyde (Polysciences) and 2.0% Formaldehyde (VWR). Samples were then dehydrated in one change each of 50%, 70%, 85%, and 95% Ethanol Solution (200 proof anhydrous Ethanol, Acros Organics, in ddH_2O) for 20 min each, then two changes of 100% Ethanol (200 proof anhydrous Ethanol, Acros Organics) for 30 min, followed by critical point drying in Hexamethyldisilizane (HDMS. Electron Microscopy) for 20 min. Samples were allowed to air dry, then were stored in a desiccator until further processing.

5.2.5 Static Seeding of Decellularized Arterial Scaffolds

Arterial scaffolds were neutralized and cannulated as in *5.2.2*. The cannulated scaffolds were then filled with ~400 μL endothelial cell solution, prepared as in *5.2.2*, and the ends were plugged with plug caps. Fibroblast solution, prepared as in *5.2.2* was pipetted onto the scaffolds with a sterile transfer pipette, ~500 μL. The scaffolds were incubated at 37°C with 5% CO_2 for 15 min. The scaffolds were rotated ~60°, seeded with more fibroblast solution, and incubated 15 more min. This was repeated a third time, then the scaffolds were incubated for 4 hours before being immersed in DMEM + 10% FBS + 1% Pen/Strep and incubated overnight. Normal and high glucose vascular bioreactors were set up as in *5.2.3* and the samples were processed as in *5.2.4*.

To analyze protein expression in the drop-seeded TEVGs, the snap-frozen samples were homogenized in 600 μL RIPA Buffer with a rotary-tip homogenizer for ~5 min. The homogenates were then centrifuged at 12,000 xg for 15 min at 4°C and the supernatants were transferred and stored at -20°C until further processing. Protein concentration was measured by BCA Assay and protein expression was measured by Western Blot using the method described in *4.2.3.1*.

To analyze cellularity, scaffold pieces were prepared for Live/Dead Cell Viability Assay for fixed and dehydrated for SEM. Dehydrated and desiccated samples were fixed to aluminum stubs using double-sided carbon tape. The stubs were sputter-coated with platinum at 10 V, 15 mA for 2 min on a Hummer® 6.2 Sputtering System (Anatech, Ltd.). Images were acquired on an S-4800 Scanning Electron Microscope (Kawasaki) at 5 kV and 1000X and 2500X magnification.

5.3 Results and Discussion

5.3.1 Analysis of Cellularity of Dynamically-Seeded Scaffolds

The drop-seeded scaffolds had very few cells anywhere on the pieces imaged after Live/Dead Assay (**Figure 5.5**). Histology using DAPI and H&E (results not shown) showed similar results. Similarly protein and RNA concentrations were too low to perform protein and mRNA expression analysis by Western Blot and RT PCR, respectively (results not shown). It is for this reason that the bioreactor experiment was repeated using the simplified seeding technique. Complications with the rotary seeding chambers may have

contributed to a lack of cells on the scaffolds prior to subjecting them to flow in the bioreactor, but experimental complications prevented examination of the scaffolds prior to starting the bioreactor.

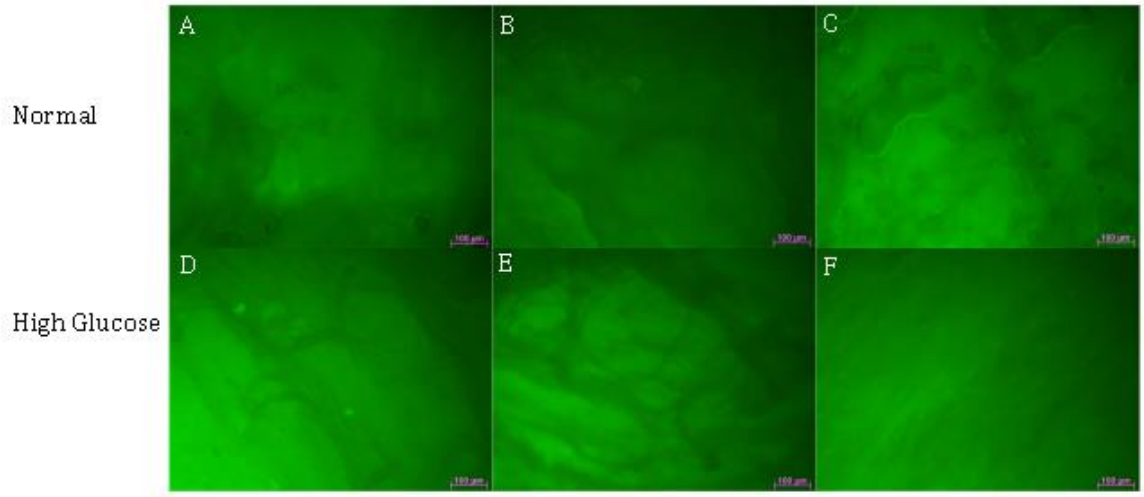

Figure 5.5: Live/Dead Cell Viability Assay of Dynamically-Seeded TEVG after Bioreactor Conditioning. Rings of the seeded scaffolds were cut from three scaffolds each from each bioreactor (normal and high glucose), cut to lie flat, and immersed in Live-Dead solution for 35 min. The scaffold pieces were placed between two slides and imaged through the thickness of the arterial scaffold wall. **A**, **B**, and **C** are samples taken from three different scaffolds conditioned in normal media. **D**, **E**, and **F** are samples taken three different scaffolds conditioned in diabetic media.

5.3.2 Analysis of Cellularity of Statically-Seeded Scaffolds

Analysis of cell viability by Live/Dead Assay on seeded scaffolds prior to starting the bioreactor failed to produce images. Rings were cut from the middle of the scaffold, then those rings were cut to lie the piece flat so that the scaffold lumen was facing up. The seeded scaffold piece was then placed between two slides to keep the piece flat. However,

this method blurred any signal produced by fluorescing cells. Gross manipulation of the scaffold while under filtered fluorescent light showed cell attachment on the scaffold, but images could not be taken. Live/Dead imaging following bioreactor conditioning (**Figure 5.6**) showed that cells were indeed retained, but coverage was inconsistent (**Figure 5.7**) and there was not a confluent layer of endothelial cells on the luminal surface, as would be required to create a totally non-thrombogenic surface. Further, retained fibroblasts were not observed on the statically-seeded scaffolds.

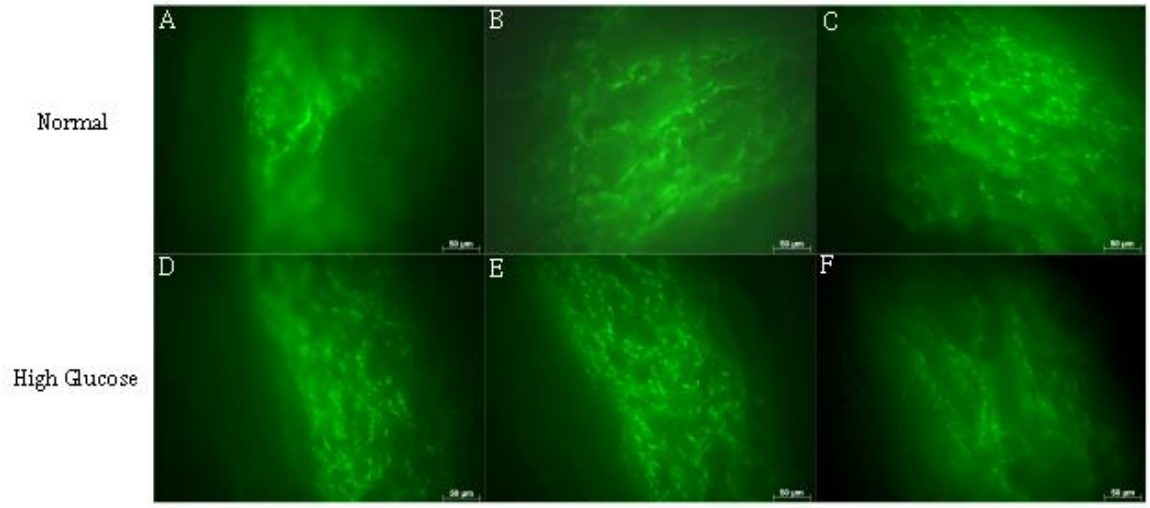

Figure 5.6: Live/Dead Cell Viability Assay of Statically-Seeded TEVG after Bioreactor Conditioning. Rings of the seeded scaffolds were cut and immersed in Live-Dead solution for 35 min. The rings were removed from the solution and placed on their side on a glass histology slide. Images are taken from above the ring. The middle portion of the image shows the luminal side of the scaffold. The left (**A**, **D**, **E**, and **F**), upper (**B**), or upper right (**C**) shows the adventitial side of the scaffold from above. **A**, **B**, and **C** are samples taken from three different scaffolds conditioned in normal media. **D**, **E**, and **F** are samples taken three different scaffolds conditioned in diabetic media.

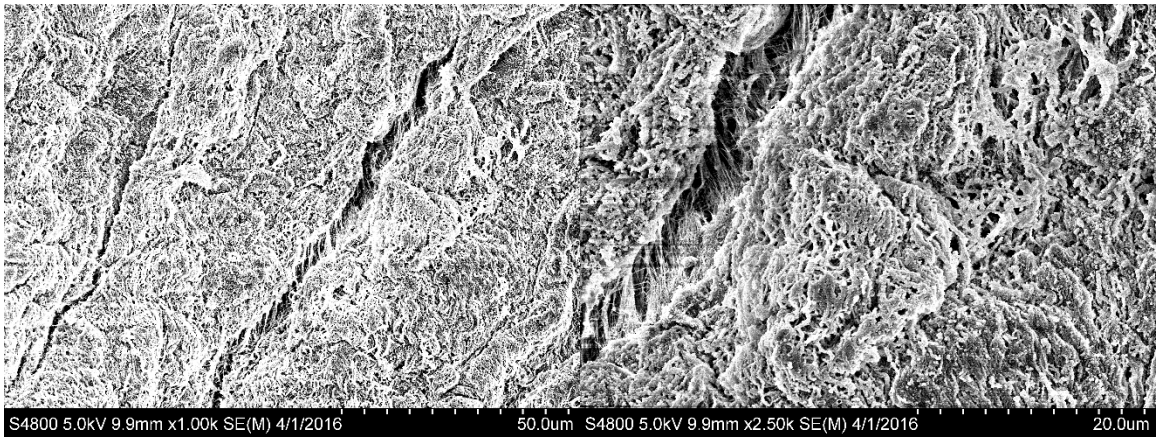

Figure 5.7: Scanning Electron Micrographs of Statically-Seeded TEVG after Bioreactor Conditioning

5.3.3 Analysis of Protein Expression

Tissue homogenates contained sufficient amounts of protein to assay by Western Blot; however, no identifiable bands were present on blots for PPARγ, NFκB, or NOX1 (**Figures A2**, **A3**, and **A4**). mTOR was upregulated in diabetic conditions (**Figure 5.7**, 1.3-fold greater expression), but not as much as in cultured hAEC for one week in diabetic conditions (3.8-fold greater expression).

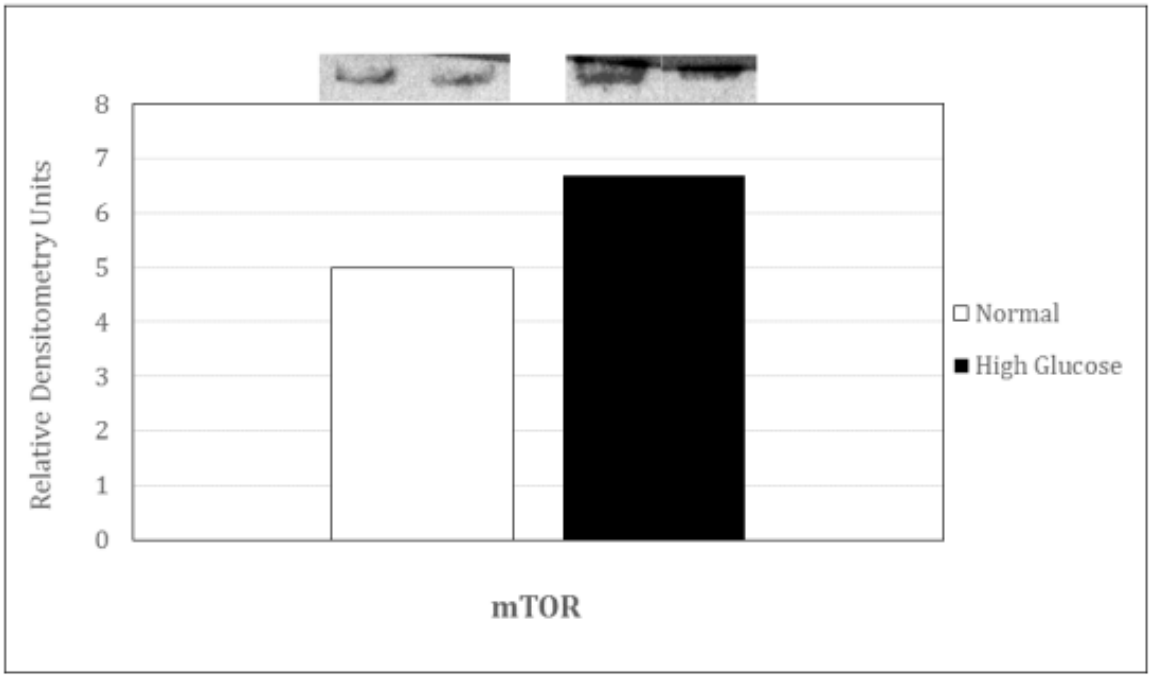

Figure 5.8: Expression of mTOR in Statically-Seeded TEVG in Normal and High Glucose Media after Bioreactor Conditioning. Bands correspond to a Mw of 250 kDa, the expected mass of the detected protein. Exposure to diabetic conditions resulted in a 1.3-fold increase in mTOR expression. N=2 for each group and 15 μg protein were used per lane

5.4 Conclusions

Achieving a confluent layer of endothelial cells has been one of the grand challenges in the field of vascular tissue engineering. Among these challenges is adherence of seeded cells to the scaffold. A vascular seeding chamber was used in these studies was used, but had some design flaws. First, the material was 3D-printed, a platform that offers low cost and easy of low-quantity manufacturing. However, the material has not held up with use and warping has caused the seal to be compromised. It can hold liquid, but it slowly leaks uncontrollably. It is the opinion of this author that enough media was lost during seeding

that cells may have starved and died before being placed in the bioreactor. Further, the design makes handling the chamber with sterile-gloved hands without compromising sterility technically challenging, and thus the opportunity to assess cell coverage on the scaffolds prior to bioreactor conditioning.

Because of the lack of cells on TEVG seeded using the seeding chambers, a simplified method for seeding was used. While not sophisticated or well controlled, this method did achieve moderation endothelialization, but did not achieve a confluent layer. This however, did demonstrate the potential of cells to adhere to this scaffold, and to remain adhered and viable under shear stress for an extended period. The small amount of cells did cause difficulty in protein expression analysis, however. Only expression of mTOR was apparent via Western Blot. The scaffolds were a small enough size and the relatively small amount of cells meant that troubleshooting and repeat experiments were impossible without simply having more samples. Curiously though, mTOR expression was increased diabetic conditions, a result that confirms what was observed 2D culture of endothelial cells in Chapter 4.

CHAPTER 6: CONCLUSIONS AND RECOMMENDATIONS FOR FUTURE WORK

6.1 Conclusions

A decellularized and PGG-stabilized vascular grafts was successfully developed. This graft is free from cells, as assessed by histological analysis, and cellular debris, as assessed by DNA content of the scaffolds. Next, the potential for endothelial-differentiated adipose derived stem cells to resist diabetic conditions was assessed. Differentiated ADSCs showed weak, but noticeable expression of endothelial markers, and show similar trends in expression to endothelial cells in normal versus diabetic conditions. This pilot study demonstrates efficacy of the differentiation protocol and a promise that differentiated ADSCs can perform well in a diabetic environment. Control of inflammation is an important problem in cardiovascular tissue engineering, so results such as these merit further investigation. Lastly, scaffolds were successfully seeded and retained cells after exposure to shear force in a bioreactor. Insufficient endothelialization is a persistent problem and perhaps the most important parameter to overcome in the field of tissue engineering, and while there was insufficient cell coverage to consider the grafts non-thrombogenic, this is a step in the right direction.

6.2 Recommendations for Future Work

Preliminary results suggest that differentiated ADSCs can mitigate transcription of inflammatory cytokines in diabetic conditions. Further cell studies should be conducted to

the degree of response in diabetic conditions. Although the glucose concentration was high, one week may be insufficient to see a wide array of effects from hyperglycemia. Cells should be cultured for 2 and 4 weeks with greater numbers of cells, then assayed to determine the longer term response of differentiated ADSCs to diabetic conditions.

One of the key hindrances in the seeding methodology is in the use of seeding chambers. 3-D printed materials have poor mechanical strength and fatigue quickly. Further, disassembly of chambers to transfer the seeded scaffolds to the bioreactor complicates an already delicate procedure. I would suggest developing a seeding chamber that can have duel functionality as a bioreactor. This could function as a mix in the design of the current bioreactor and other small bioreactors, such as the 3DKube® sold by Kiyatec, Inc. Such a seeding chamber could house a single (or multiple in the case of renal branches) arterial scaffold that could then be attached to the existing bioreactor setup without need to transfer the arteries from one chamber to another. Further, this would allow for easier upscale of studies, which is a limiting factor in the current bioreactor design.

Finally, a subsequent bioreactor study should be performed using growth factor-differentiated ADSCs. The scaffolds should be seeded in the same manner as endothelial cells and fibroblasts and conditioned for 4 weeks in normal or high glucose. The seeded scaffolds should then be assayed for the same metabolic and inflammatory markers as endothelial cell and fibroblast-seeded scaffolds to determine the 3D *in vitro* resistance of ADSC-seeded scaffolds to damage caused by diabetic inflammation.

REFERENCES

1. Abdelwahed, A. I. Bouhel, I. Skrandrani, K. Valenti, M. Kadri, P. Guiraud, R. Steiman, A.M Mariotte, K. Chedira, F. Laporte, M.G. Dijoux-Franca, and L. Chekir-Ghedira. Study of antimutagenic and antioxidant activities of gallic acid and 1,2,3,4,6-pentagalloylglucose from Pistacia lentiscus. Chemico-Biol. Interactions. 165:1-13, 2007.
2. American Diabetes Association. Economic costs of diabetes in the U.S. in 2012. Diabetes Care. 36:1033-46, 2013.
3. Badylak, S.F. The extracellular matrix as a biologic scaffold material. Biomaterials. 28:3587-93, 2007.
4. Beckman, J.A., M.A. Creager, and P. Libby. Diabetes and atherosclerosis: epidemiology, pathophysiology, and management. JAMA. 287:2570-81, 2002.
5. Brownlee M. The pathobiology of diabetic complications: a unifying mechanism. Diabetes. 54:1615-25, 2005.
6. Bunnell, B.A., M. Flaat, C. Gagliardi B. Patel, and C. Ripoll. Adipose-derived stem cells: isolation, expansion, and differentiation. Methods. 45:115-20, 2008.
7. Chavakis, E. and S. Dimmeler. Homing of progenitor cells to ischemic tissues. Antioxid. Redox. Sign. 15:967-80, 2010.
8. Chlupac, J., E. Filova, and L. Bacakova. Blood vessel replacement: 50 years of development and tissue engineering paradigms in vascular surgery. Physiol. Res. 2:119-39, 2009.
9. Chow, J.P., D.T. Simionescu, H. Warner, B. Wang, S.S. Patnaik, J. Liao, and A. Simionescu. Mitigation of diabetes-related complications in implanted collagen and elastin scaffolds using matrix-binding polyphenol. Biomaterials. 34:685-695, 2013.
10. Crapo, P.M., T.W. Gilbert, and S.F. Badylak. An overview of tissue and whole organ decellularization processes. Biomaterials. 32:3233-43, 2011.
11. De Caterina, R., M. Massaro, and P. Libby. “Endothelial functions and dysfunction” In: Endothelial Dysfunctions and Vascular Disease, edited by R. De Caterina and P. Libby. Malden, MA: Wiley-Blackwell, 2008, pp. 3-25.
12. De Francesco, F., G. Ricci, F. D’Andrea, G.F. Nicoletti, and G.A. Ferraro. Human adipose-derived stem cells: from bench to bedside. Tissue Eng. PT-B: Rev. 21:572-84, 2015.
13. Fattori, R. and T. Piva. Drug-eluting stents in vascular intervention. Lancet. 361:247-9, 2003.
14. Fercana, G., D. Bowser, M. Portilla, E.M. Langan, C.G. Carsten, D.L. Cull, L.N. Sieard, and D.T Simionescu. Tissue Eng. PT-C: Methods. 20:1016-27, 2014

15. Fischer, L.J., S. McIlhenny, T. Tulenko, N. Golesorkhi, P. Zhang, R. Larson, J. Lombardi, I. Shapiro, and P.J. DiMuzio, J. Surg. Res. 152:157-66, 2009.
16. Gentile, P., A. Orlandi, M.G. Scioli, C. Di Pasquali, I. Bocchini, and V. Cervelli. Concise review: adipose-derived stromal vascular fraction cells and platelet-rich plasma: basic and clinical implications for tissue engineering therapies in regenerative surgery. Stem Cells Trans. Med. 1:230-6, 2012.
17. Huang, A.H., and L.E. Niklason. Engineering of arteries in vitro. Cell. Mol. Life Sci. 71:2103-18, 2014.
18. International Diabetes Foundation. Annual Report 2014. 2014.
19. Jukema, J.W., J.W. Verschuren, T.A.N. Ahmed, and P.H.A. Quax. Restenosis after PCI: part I: pathophysiology and risk factors. Nat. Rev. Cardiol. 9:53-62, 2012.
20. Kayama, Y., U. Raaz, A. Jagger, M. Adam, I. Schellinger, M. Sakamoto, H. Suzuki, K. Toyama, J.M. Spin, and P.S. Tsao. Diabetic cardiovascular disease induced by oxidative stress. Int. J. Mol. Sci. 16:25234-63, 2015.
21. Krawiec, J.T. and D.A. Vorp. Adult stem cell-based tissue engineered blood vessels: a review. Biomaterials. 33:3388-400, 2012.
22. Libby, P., P.M. Ridker, and G.K. Hansson. Inflammation in atherosclerosis: from pathophysiology to practice. J. Am. Coll. Cardiol. 54:2129-38, 2009.
23. Lombardo, E., O. DelaRosa, R. Mancheno-Corvo, R. Menta, C. Ramirez, and D. Buscher. Toll-like receptor-mediated signaling in human adipose-derived stem cells: implications for immunogenicity and immunosuppressive potential. Tissue Eng. PT-A. 15:1572-89, 2009.
24. Maitra, A. "The endocrine system." In: Robbins and Cotran Pathologic Basis of Disease, edited by V. Kumar, A.K. Abbas, and J.C. Aster. Philadelphia: Elsevier-Saunders, 2015, pp. 1073--139.
25. Marshall, S. Role of insulin, adipocyte hormones, and nutrient-sensing pathways in regulating fuel metabolism and energy homeostasis: a nutritional perspective of diabetes, obesity, and cancer. Sci Signal. 346:1-10, 2006.
26. McKinley, M. and V.D. O'Loughlin. Human Anatomy. New York: McGraw-Hill, 2012.
27. Mitchell, R.N. "Blood vessels." In: Robbins and Cotran Pathologic Basis of Disease, edited by V. Kumar, A.K. Abbas, and J.C. Aster. Philadelphia: Elsevier-Saunders, 2015, pp. 483-522.
28. Mozaffarian, D., et al. Heart disease and stroke statistics-2015 update. Circulation. 131:e29-e322, 2015.
29. National Center for Chronic Disease Prevention and Health Promotion. National diabetes statistics report, 2014. Centers for Disease Control and Prevention. 2014.

30. Negre-Salvayre, A., R. Negre-Salvayre, N. Auge, R. Pamplona, and M. Portero-Otin. Hyperglycemia and glycation in diabetic complications. Antioxid. Redox. Sign. 11:3071-109, 2009.
31. Nguyen, L.L. Percutaneous treatment of peripheral vascular disease: the role of diabetes and inflammation. J. Vasc. Surg. 45:Supp A:A149-57, 2007.
32. Pashneh-Tala S., S. MacNeil, and F. Claeyssens. The tissue-engineered vascular graft - past, present, and future. Tissue Eng. PT B-Rev. 00:1-33, 2015.
33. Peck, M. D. Gebhart, N. Dussere, T.N. McAllister, and N. L'Heureux. The evolution of vascular tissue engineering and current state of the art. Cells Tissues Organs. 195:144-58, 2012.
34. Pober, J.S., W. Min, and J.R. Bradley. Mechanisms of endothelial dysfunction, injury, and death. Annu. Rev. Pathol. Mech. Dis. 4:71-95, 2009.
35. Ross, R. Atherosclerosis-an inflammatory disease. N. Engl. J. Med. 340:115-26, 1999.
36. Seifu, D.G., A. Purnama, K. Mequanint, and D. Mantovani. Small-diameter vascular tissue engineering. Nat. Rev. Cardiol. 10:410-21, 2013.
37. Simionescu, A., J.B. Schulte, G. Fercana, and D.T. Simionescu. Inflammation in cardiovascular tissue engineering: the challenge to a promise: a minireview. Int. J. Inflamm. 2011:1-11, 2011.
38. Sinha, A., N. Nasoudi, and N. Vyavahare. Elast-restorative properties of polyphenols. Biochem. Biophys. Res. Co. 444:205-11, 2014.
39. Sitia, S., L. Tomasoni, F. Atzeni, G. Ambrosio, C. Cordiano, A. Catapano, S. Tramontana, F. Perticone, P. Naccarato, P. Camici, E. Picano, L. Cortigiani, M. Bevilacqua, I. Milazzo, D. Cusi, C. Barlassina, P. Sarzi-Puttini, and M. Turiel. From endothelial dysfunction to atherosclerosis. Autoimmun. Rev. 9: 830-4, 2010.
40. Stirban, A., T. Gawlowski, and M. Roden. 2 Vascular effects of advanced glycation endproducts: clinical effects and molecular mechanisms. Mol. Metabolism. 3:94-108, 2013.
41. Tiwari, D.K., K.B. Pandey, A.B. Abidi, S.I. Rizvi. Markers of Oxidative Stress during Diabetes Mellitus. J. Biomarkers 2013, 1-8.
42. Xu, S., M. Bendeck, and A.I. Gotlieb. "Vascular pathobiology: atherosclerosis and large vessel disease." In: Cardiovascular Pathology, edited by J. Butany and M.L. Buja. London: Elsevier-Academic Press, 2016, pp. 85-124.
43. Yahagi, K., F.D. Kolodgie, F. Otsuka, A.V. Finn, H.R. Davis, M. Joner, and R. Virmani. Pathophysiology of native coronary, vein graft, and in-stent atherosclerosis. Nat. Rev. Cardiol. 13:79-98, 2016.
44. Zhang, J.H., L. Li, S.H. Kim, A.E. Hagerman, and J.X. Lu. Anti-cancer, anti-diabetic, and other pharmacologic and bioactivities of penta-galloyl-glucose. Pharm. Res. 26:2066-80, 2009.

APPENDICES

Appendix A - Supplementary Figures

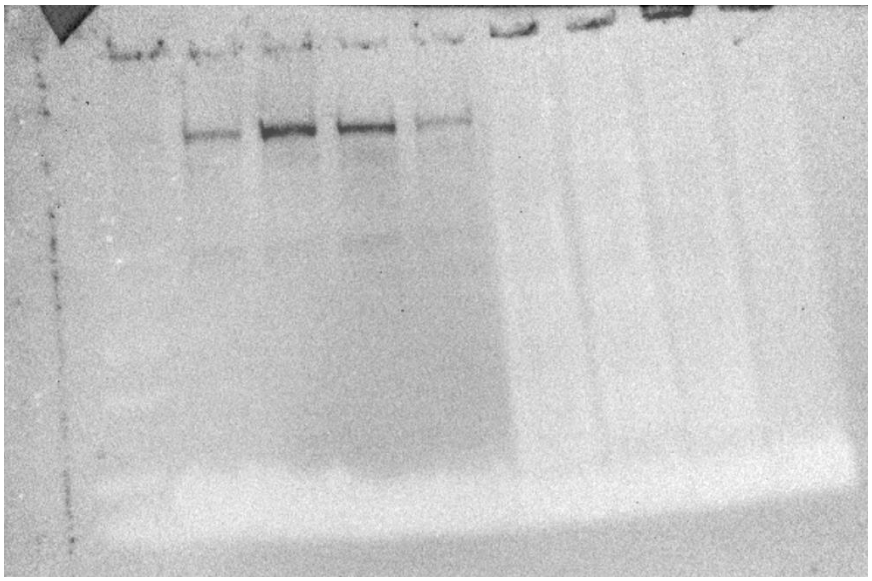

Figure A1: Western Blot for mTOR. Lane 1 = Ladder; Lane 2 = Differentiated hADSC in normal glucose media; Lane 3 = Differentiated hADSC in high glucose media; Lane 4 = hAEC in high glucose media; Lane 5 = hAEC in normal glucose media; Lane 6 and 7 = Statically-seeded scaffolds conditioned in normal glucose media in vascular bioreactor; Lane 8 and 9 = Statically-seeded scaffolds conditioned in high glucose media in vascular bioreactor; N=3, pooled for Lanes 2-5; N=1 for Lanes 6-9; 15 μg protein per lane

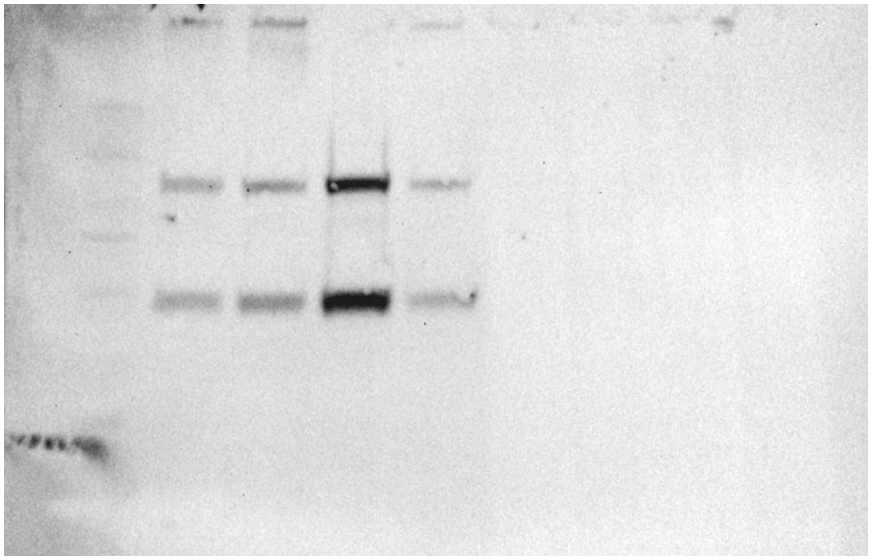

Figure A2: Western Blot for NFκB. Lane 1 = Ladder; Lane 2 = Differentiated hADSC in normal glucose media; Lane 3 = Differentiated hADSC in high glucose media; Lane 4 = hAEC in high glucose media; Lane 5 = hAEC in normal glucose media; Lane 6 and 7 = Statically-seeded scaffolds conditioned in normal glucose media in vascular bioreactor; Lane 8 and 9 = Statically-seeded scaffolds conditioned in high glucose media in vascular bioreactor; N=3, pooled for Lanes 2-5; N=1 for Lanes 6-9; 15 μg protein per lane

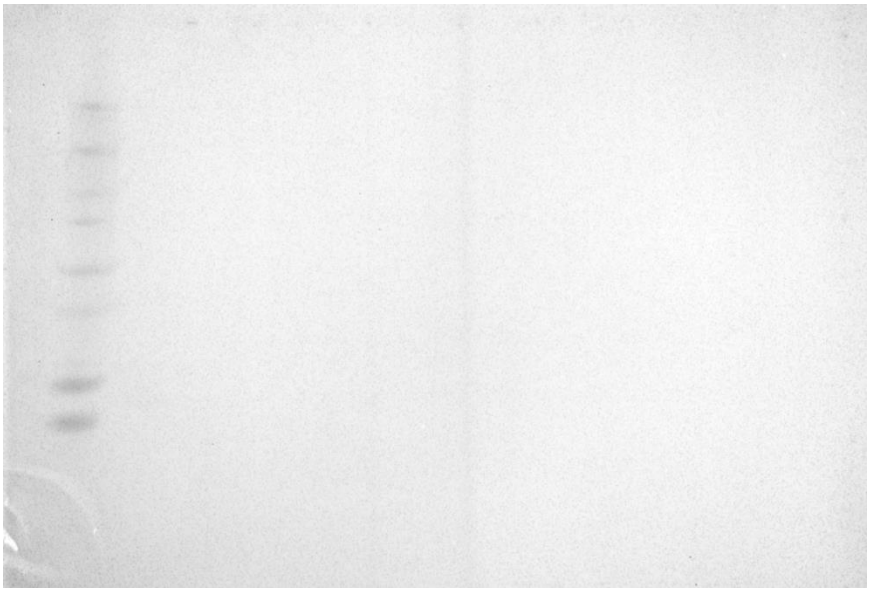

Figure A3: Western Blot for NOX1. Lane 1 = Ladder; Lane 2 = Differentiated hADSC in normal glucose media; Lane 3 = Differentiated hADSC in high glucose media; Lane 4 = hAEC in high glucose media; Lane 5 = hAEC in normal glucose media; Lane 6 and 7 = Statically-seeded scaffolds conditioned in normal glucose media in vascular bioreactor; Lane 8 and 9 = Statically-seeded scaffolds conditioned in high glucose media in vascular bioreactor; N=3, pooled for Lanes 2-5; N=1 for Lanes 6-9; 15 μg protein per lane

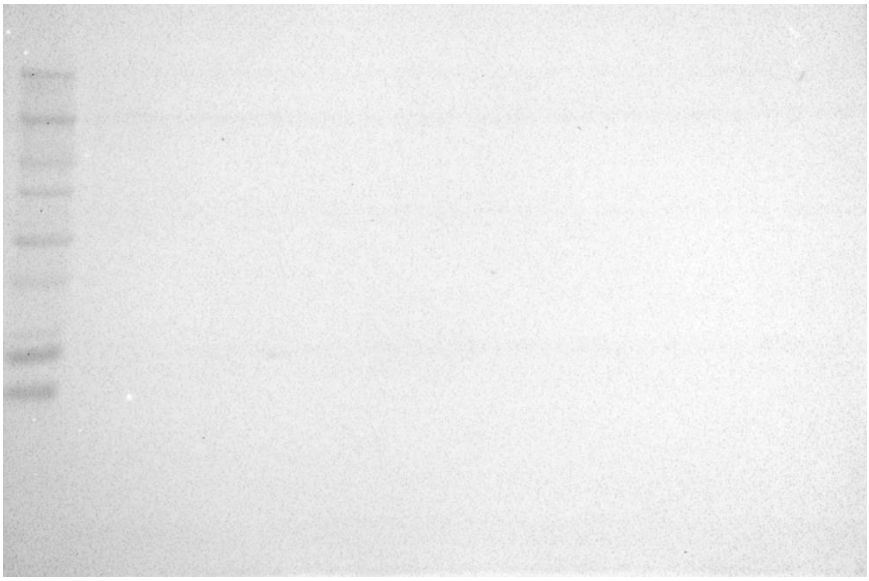

Figure A4: Western Blot for PPARγ. Lane 1 = Ladder; Lane 2 = Differentiated hADSC in normal glucose media; Lane 3 = Differentiated hADSC in high glucose media; Lane 4 = hAEC in high glucose media; Lane 5 = hAEC in normal glucose media; Lane 6 and 7 = Statically-seeded scaffolds conditioned in normal glucose media in vascular bioreactor; Lane 8 and 9 = Statically-seeded scaffolds conditioned in high glucose media in vascular bioreactor; N=3, pooled for Lanes 2-5; N=1 for Lanes 6-9; 15 μg protein per lane

Appendix B - Supplementary Tables

Sample Conditions	Sample	Concentration (μg/μL)
Differentiated ADSC in Normal Glucose Media	A1NP	1.319
	A2NP	1.319
	A3NP	1.395
Differentiated ADSC in High Glucose Media	A1DP	2.269
	A2DP	1.877
	A3DP	1.395
Endothelial Cells in Normal Glucose Media	E1NP	1.299
	E2NP	2.561
	E3NP	1.683
Endothelial Cells in High Glucose Media	E1DP	3.459
	E2DP	3.701
	E3DP	3.632

Table A1: Protein Concentration of Cell and Tissue Lysates. For Western Blots, 5 μg of each sample was pooled for each lane.